

The University of Maine

DigitalCommons@UMaine

---

Honors College

---

Spring 2023

## A Study on Scaling Floating Offshore Wind Turbine Geometry and Hydrostatics with Increasing Turbine Size

Samuel Davis

Follow this and additional works at: <https://digitalcommons.library.umaine.edu/honors>



Part of the [Ocean Engineering Commons](#)

---

This Honors Thesis is brought to you for free and open access by DigitalCommons@UMaine. It has been accepted for inclusion in Honors College by an authorized administrator of DigitalCommons@UMaine. For more information, please contact [um.library.technical.services@maine.edu](mailto:um.library.technical.services@maine.edu).

A STUDY ON SCALING FLOATING OFFSHORE WIND TURBINE GEOMETRY  
AND HYDROSTATICS WITH INCREASING TURBINE SIZE

by

Samuel Davis

A Thesis Submitted in Partial Fulfillment  
of the Requirements for a Degree with Honors  
(Mechanical Engineering)

The Honors College

University of Maine

May 2023

Advisory Committee:

Andrew Goupee, Associate Professor of Mechanical Engineering, Advisor  
Richard Kimball, Professor of Mechanical Engineering  
Amrit Verma, Assistant Professor of Mechanical Engineering

Copyright 2023 Davis  
All Rights Reserved

## ABSTRACT

Floating offshore wind offers a clean and sustainable alternative to fossil fuels for the future of energy production. In Maine in particular, there is a great opportunity to take advantage of the wind resource off the coast and become a global leader in offshore wind. With the Maine coastal waters being too deep for fixed-bottom turbine structures, floating platforms that support the turbines have the opportunity to gain traction as the technology matures. As wind turbines increase in size and capacity, the floating hulls must also increase in size. The research presented in this thesis aimed to calculate and examine trends of floating offshore wind turbine floating hulls as turbine size increased. A mathematical model based on the University of Maine's VoltturnUS-S semi-submersible hull design, was developed to search for a minimum mass hull design that met specific constraints to approximate a viable design. Multiple studies were performed to examine the geometry trends, constraint trends, and relative costs of the designs given different constraints. The model showed that with constraints similar to current real-world designs, the relative cost of the hull per unit power of the turbine is relatively constant, while changing the constraints put on the system can yield more cost-efficient designs. The results of the studies provided a general outlook for the future of floating offshore wind hull designs, given different frameworks to determine how designs may be able to evolve.

## ACKNOWLEDGEMENTS

I would like to thank my honors thesis advisor, Dr. Andrew Goupee, for his guidance and the wealth of knowledge that he has shared throughout the course of this research.

Thank you also to my committee members, Dr. Richard Kimball, and Dr. Amrit Verma. Dr. Kimball's class on floating systems design and Dr. Verma's class on offshore wind farm design have taught me so much about this field and strengthened my excitement for future work.

I would also like to thank all the faculty and staff from the Department of Mechanical Engineering and the Honors College, who have made my time as an undergraduate at the University of Maine exceptionally enjoyable and enlightening.

## TABLE OF CONTENTS

INTRODUCTION	1
Purpose	2
LITERATURE REVIEW	3
METHODOLOGY	8
Model Introduction	8
Turbine Scaling	9
Hull Scaling	11
Constraints	20
Initial Tuning	21
RESULTS	22
Problem Overview	22
Defining Constraints	22
Model Verification	23
Platform Mass Trends	25
Platform Geometry Trends	26
Constraint Trends	29
Relative Cost	32
DISCUSSION	34

Study One: Baseline Constraints	34
Study Two: Expanded Hull Maximum Width	35
Study Three: Bottom Beam Height Constraint Removed	36
Comparison of Studies	39
Limitations	39
CONCLUSION	42
Findings	42
Research Significance and Contributions	44
Future Research	44
BIBLIOGRAPHY	45
APPENDIX A: SCALING EQUATIONS	49
APPENDIX B: DNV ADDED MASS GUIDE	50
APPENDIX C: MODEL MATLAB CODE	51
AUTHOR'S BIOGRAPHY	59

## TABLE OF FIGURES

Figure 1. VoltturnUS-S coordinate system	8
Figure 2. Components of a wind turbine	10
Figure 3. VoltturnUS hull geometry	13
Figure 4. Minimum mass vs. turbine size	26
Figure 5. Radial column diameter and radial spacing vs. turbine size	27
Figure 6. Maximum floater width vs. turbine size	28
Figure 7 Bottom beam height vs turbine size	29
Figure 8. Pitch and heave natural periods vs. turbine size	30
Figure 9. Pitch deflection vs. turbine size	31
Figure 10. Tow-out draft vs. turbine size	32
Figure 11. Mass per megawatt vs. turbine size	33
Table 1. Symbolic model constraints	21
Table 2. Hull constraints	23
Table 3. Model comparison with reference	24
Table 4. Percent error of model relative to VoltturnUS-S reference	24
Table 5. Study two: percent decrease in mass relative to study one	36
Table 6. Study three: percent decrease in mass relative to study one	37



## INTRODUCTION

Offshore wind power generation offers higher wind speeds and more consistent winds than those on land. As the world shifts towards clean energy methods to combat the global climate change crisis, offshore wind is in a position to become an important piece of the new age of energy generation. Offshore wind farms have been commissioned in Europe for over two decades, but the first offshore wind farm in the United States did not begin operations until 2016 [1]. While offshore wind is still a relatively novel technology in the United States, the knowledge from European projects and a recent increase in commercial interest has offshore wind primed to experience large growth.

Offshore wind farms are traditionally constructed using fixed-bottom structures that are in direct contact with the ocean floor [2]. In areas with deep waters, such as the Gulf of Maine, fixed bottom structures are not viable, so floating structures are developed to support the wind turbines. The technology and knowledge within the floating offshore wind industry has been rapidly advancing in recent years, and with this growth has come an increase in the power capacity of offshore wind turbines. With 15-megawatt (MW) turbines approaching the expected norm, the near future may include turbines of 20 MW capacity and beyond. This study aims to calculate and observe trends of key floating offshore wind turbine (FOWT) system characteristics as the turbine scale increases. To perform this study, the University of Maine (UMaine) VoltturnUS-S reference floating offshore wind turbine semi-submersible designed for the International Energy Agency (IEA)-15-240-RWT 15MW reference wind turbine was used as a baseline for developing a mathematical model to investigate the scaling effects of large floating wind turbines.

## Purpose

This study aims to generate key parameters of a FOWT hull given the wind turbine power capacity and a range of geometric inputs for the floating foundation. The FOWT floating foundations with the minimum mass that meets the constraints outlined in the model will be identified so that the geometric inputs can be recorded. The geometric features of the floating foundation will be determined through optimal system parameters from a given range of geometric values. The minimum mass FOWT hulls at a range of wind turbine sizes will then be compared to observe trends and system behavior as turbine size increases. Different constraint values will be used in the model to create multiple study cases to observe how those constraints generate different minimum mass FOWT systems.

## LITERATURE REVIEW

The United States is currently in the early stages of offshore wind development on a commercial scale [1]. As the need for renewable energy increases across the globe, offshore wind has emerged as a leading option for clean energy production in coastal areas of the United States, particularly in the Gulf of Maine. Fixed-bottom offshore wind turbines typically operate at water depths up to fifty meters. The Gulf of Maine has water depths of approximately sixty meters at three nautical miles offshore, with 89% of the available wind resource located in deep waters [3]. Floating wind technology is needed to harness the more than 156 GW available in the Gulf of Maine, as well as the wind resource available in deep-water areas across the globe.

In September 2022, the Biden-Harris Administration announced actions to expand offshore wind energy, with a goal of deploying 20 GW of offshore wind by 2030. Included in this initiative is the goal of 15 GW of floating offshore wind capacity by 2035 [4]. Over the past decade, there have been several floating wind foundation concepts in various demonstration and pre-commercial phases. The floating foundation concepts allow for the prospect of deep-water offshore wind installations along with standardized production of foundations to be used commercially [5].

With the offshore wind market set to see rapid growth in the coming decade, the offshore wind industry is pushing for increased generating capacity to lower project costs. Offshore wind turbine original equipment manufacturers (OEMs) are competing to deliver turbines with increasing power capacities to lower the number of turbines needed for offshore wind farms. Current turbine capacities for offshore wind are in the range of

7-8 MW, with expected projects in the 10-11 MW range. Major turbine OEMs have announced plans for turbines with a 15 MW turbine capacity, and this number is expected to increase as technology continues to evolve and improve [1]. The median turbine power capacity used in 2035 is currently expected to be up to 17 MW according to some estimates [6]. Turbine power capacities are expected to continually increase for the foreseeable future, so keeping this in mind for the future of floating offshore wind systems is vital in the advancement of the technology.

As the power capacity of offshore wind turbines increases, the floating foundations also must increase in size to accommodate. There are many constraints on the increasing size of the floating foundations, many of which are defined by the ports available for the construction and maintenance of the FOWT systems [7]. Constraints on the draft of the foundation while in port, as well as the overall geometric size of the foundation are vital in ensuring that the foundations can be constructed and transported in the port [8]. The size constraints on the hull also play a vital role in the transportation of the structure, whether that be from one port to another, or out to the site of installation. These values are important parameters in the calculation of the hydrostatic properties of the foundation, so must be taken into consideration during the design.

As the scale of offshore floating wind systems increases, it is important that there is a procedure developed to analyze the effects of the increasing size. A major part of this procedure is the determination of important hydrostatic and hydrodynamic parameters. On a basic level, these parameters include stability determinations, frequency-dependent hydrodynamic parameters, natural periods, motion response, and nominal pitch displacement. Important hydrostatic parameters can be determined with relatively simple

numerical models, while hydrodynamic analysis can require more advanced simulation tools [9]. These parameters determine the viability of floating foundation designs with chosen wind turbine sizes and allow for the analysis of trends as turbine sizes increase. The hydrostatic parameters of a FOWT system vary greatly depending on the type of foundation that is used.

Detailed specifications of commercial wind turbines are rarely shared with the public, so reference turbines created by research institutions are used for the further development of offshore wind technology [10-18]. Many of the detailed specifications of floating offshore wind floaters are also protected from public knowledge, so the University of Maine developed a reference platform, the VoltturnUS-S semisubmersible to support the IEA-15-240-RWT 15 MW reference wind turbine [19]. In a technical report released by the National Renewable Energy Laboratory (NREL), all the detailed specifications and properties of the VoltturnUS-S platform are outlined to aid in the research and development of floating offshore wind technology. The VoltturnUS-S design can be used as a reference for observing the trends of FOWT systems as the scale of turbine power capacity increases.

There are four main types of FOWT foundations: spar, tension-leg platform, semi-submersible, and barge. Semi-submersible floating wind foundations are typically characterized by multiple columns connected by structural members [20]. The wind turbines sit on one of the columns, typically the center column such as in the VoltturnUS-S foundation. The stability of the foundation is provided by the water-plane area of the columns. Semi-submersible foundations have relatively lesser drafts when compared to other foundations, and water ballast located in the columns allows for the variability of

draft between quayside, towing, and operational conditions. A key feature of the design process of semi-submersible foundations is the ability to tune the geometry of the columns and their spacing to address wave forcing and their associated periods.

There have been many approaches to scaling offshore wind turbines and floating foundations [21]. Scaling the wind turbines has been done by applying scaling laws determined in literature based on structural and aerodynamic factors, as well as analyzing commercial data and determining scaling trends. The scaling of the floating foundation has been done in a similar way, using derived scaling laws to determine the platform geometry and mass properties, which can then be used to determine more complex parameters of the system. Wu (2021) used scaling laws to upscale the OC4 DeepCWind semi-submersible [22] from 5 MW to 10 MW, and 15 MW using data from reference turbines at each scale. The 15 MW OC4 was then compared to the VoltturnUS-S system.

Scaling laws have been developed for floating offshore wind systems based on trends of current and proposed technologies [23]. Sergiienko et al. (2022) examined the specifications of nine reference offshore wind turbines that ranged between 1.5 MW and 20 MW in rated power. The values of parameters across the range of reference turbines were plotted and fit with equations using the best power fit and heuristic engineering approach using rotor diameter as the independent variable. The result of these trends showed that wind turbine mass, rated power, and thrust force scaled close to the square of the rotor diameter. Proposed floating semi-submersible platforms were then reviewed. It was determined that the platform design is driven by a strong correlation between the rotor diameter and the product of the radius to the offset column and the offset column diameter. It was also observed that the draft as well as the pitch and heave natural periods

remained similar for all the reference platforms despite the difference in turbine sizes. The draft was kept close to 20 meters, while the pitch and heave natural periods were observed to be about 30 seconds and 20 seconds respectively.

Sergiienko et al. then went on to review and compare platform scaling laws outlined by previous literature. Three main methods of scaling laws were explored: power, mass, and fixed-draft. It was determined that the fixed-draft scaling law may be the closest to existing trends because platform developers seem to be keeping draft at about 20 meters as turbine size increases, but this method results in higher motion amplitudes in all degrees of freedom. The mass scaling procedure was recommended as the better starting point for platform design due to lack of increased motions using this method. The scaling laws can provide a baseline estimate for the increase in geometric and mass properties when calculating the actual value may be too complex or unachievable. Using the scaling trends also allow for a comparison of the current systems and how they relate to each other, as well as providing an estimate on how overall system properties will trend as turbines get larger.

## METHODOLOGY

### Model Introduction

The scalable hydrostatic model of the VoltturnUS-S system started with the baseline system properties defined in the reference document created by the University of Maine and NREL [19]. The floating offshore wind system properties, key components, geometry, and mass properties of the model are all based on the values for the VoltturnUS-S. From the baseline values, scaling laws are applied to analyze key parameters of the system. The VoltturnUS-S system is shown in Figure 1, with the reference coordinate system used in for analysis.

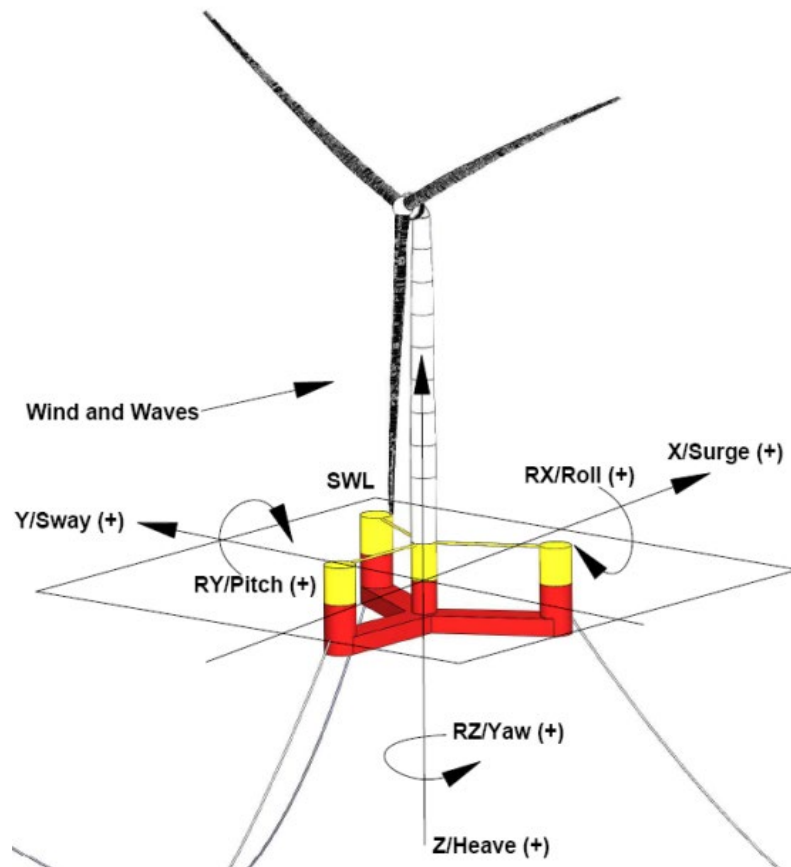


Figure 1. VoltturnUS-S coordinate system

Source: Adapted from [10]



## Turbine Scaling

The power capacity of the turbine, and the key geometric features of the VoltturnUS-S floating foundation are input into the model to set the parameters of the model analysis. Scaling law trends described by Sergiienko et al. [23] were used to relate turbine power capacity to rotor diameter, and then rotor diameter to mass properties of the tower, nacelle, and rotor for the turbine, as well as the steel and concrete ballast mass in the floater. Appendix A provides the full table of turbine scaling law equations.

The rated power of the turbine is scaled as a function of the rotor diameter as shown in Equation 1.

$$P = 821D^{1.79} \text{ (MW)} \quad (1)$$

where  $D$  is the rotor diameter in meters and  $P$  is the turbine power in MW. Equation 1 can be manipulated to solve for rotor diameter, with turbine power being input into the function based on a user-defined value. Once the rotor diameter is determined based on the initial scaling law, other key parameters of the turbine can be calculated using other scaling law trends.

The peak thrust is calculated using Equation 2.

$$F_T = 84D^{1.86} \text{ (kN)} \quad (2)$$

where  $F_T$  is the peak thrust experienced by the turbine in kilonewtons (kN). Thrust is the axial load experienced by the turbine rotor. Peak thrust is an estimation of the maximum thrust load that the turbine would experience during operation. The peak thrust typically occurs at the turbines rated wind speed.

The geometric and mass scaling of the wind turbine was also calculated using empirical scaling laws. The key components of the wind turbine are shown in the diagram Figure 2.

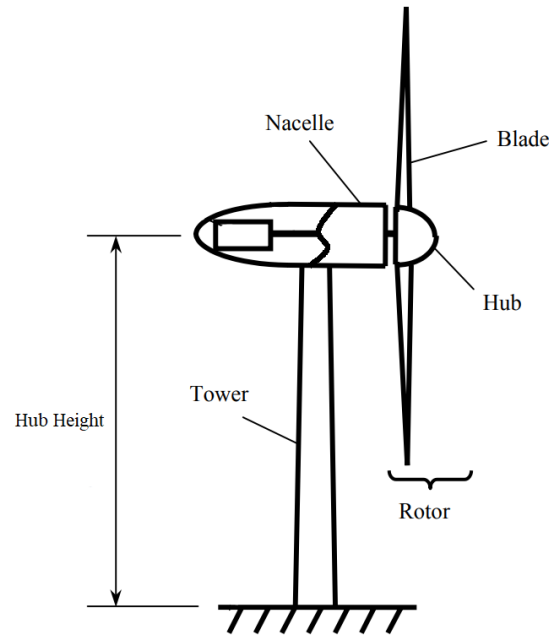


Figure 2. Components of a wind turbine

Source: Adapted from [24]

The hub height of the turbine is calculated using Equation 3.

$$z_{hub} = 84D^{1.86} \text{ (m)} \quad (3)$$

where  $z_{hub}$  is the hub height of the wind turbine in meters. Hub height is the distance from the water line to the center of the turbine rotor.

The tower diameter is calculated using Equation 4.

$$D_{tower} = 0.23D^{0.68} \text{ (m)} \quad (4)$$

where  $D_{tower}$  is the outside diameter of the turbine tower. For simplification, the tower was assumed to be the same diameter for its entire length.

The scaling equation described by Sergiienko et al. for the turbine tower was based on onshore turbine properties, thus being an underestimation of the actual tower mass. To achieve a closer approximation, the turbine tower mass was scaled according to the  $p$  scale factor described in the Hull Scaling section below. The reference mass used in the calculation came from the mass of the turbine tower in the VoltturnUS-S reference document. Equation 5 shows the tower mass calculation.

$$m_{tower} = m_{tower,ref} \cdot p^2 \quad (5)$$

The masses of the turbine hub, rotor, and nacelle are given by Equations 6, 7, and 8, respectively.

$$m_{hub} = 0.23D^{2.46} \text{ (kg)} \quad (6)$$

$$m_{rotor} = 5D^{2.05} \text{ (kg)} \quad (7)$$

$$m_{nacelle} = 24.3D^{1.88} \text{ (kg)} \quad (8)$$

The mass of the rotor and nacelle are combined to calculate the mass of the rotor-nacelle-assembly (RNA), which is defined as  $m_{RNA}$ .

### Hull Scaling

To get initial values for the for the masses of the floating platform, scaling laws were used based on a fixed draft assumption. The fixed draft scaling law was used to preserve the mass properties of the system while maintaining a similar draft to meet port and transportation limitation. There are two scale factors used in this model. Scale factor

$s$  is used to scale the wind energy system, and scale factor  $p$  is used to scale the floating platform. The equation that defines  $p$  for fixed draft scaling laws is given by Equation 9.

$$p = \sqrt{\frac{m_{scaled}}{m_{base}}} = s \quad (9)$$

where  $m_{scaled}$  is the scaled mass of the floating platform and  $m_{base}$  is the baseline mass of the platform.

The value of  $s$  is the ratio between the scaled rotor diameter to the baseline rotor diameter, as shown in Equation 10.

$$s = \frac{D_{scaled}}{D_{base}} \quad (10)$$

where  $D_{scaled}$  is the scaled rotor diameter calculated using Equation 1, and  $D_{base}$  is the baseline rotor diameter. Using the value calculated in Equation 10, the value  $m_{scaled}$  can be solved for using Equation 9.

The scaled fixed foundation mass is calculated using Equation 9, which includes the platform steel mass, and the fixed concrete ballast. The total fixed system mass includes the fixed foundation mass, as well as the mass of the turbine RNA and tower. The total fixed system mass is used as the minimum tow-out draft for this analysis. The scaled fixed concrete ballast mass and the foundation steel mass are individually calculated by maintaining the same ratio of mass to the overall fixed foundation mass that is defined in the baseline system.

The scaled mass properties of the hull are combined with the geometry to achieve a detailed model of the system. The geometry of the floating foundation is determined by the user input values for key features such as the column diameters, radial spacing,

bottom beam height, installed draft, freeboard, and position of fairlead connection. The key geometric features of the VoltturnUS-S floating foundation are labeled in Figure 3.

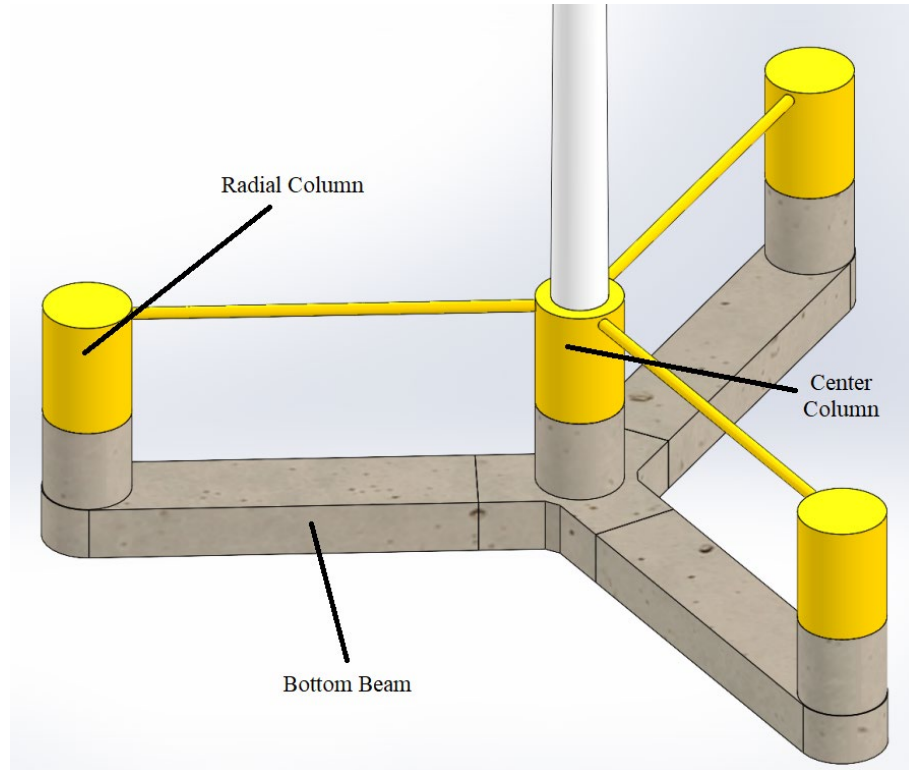


Figure 3. VoltturnUS hull geometry

The center and radial columns are cylinders with defined radii, and heights determined by the draft and freeboard. The bottom beams are rectangular prisms with defined heights, lengths determined by the radial spacing and the column radii, and widths defined as the radial column diameter. The volume of the water displaced by the foundation was determined based on the geometric dimensions of the key foundation features, as well as the defined installed draft. The equations for the displaced volumes of the center column, the three radial columns, and bottom beam, and total displaced volume are shown by Equations 11, 12, 13, and 14, respectively.

$$V_{CC,disp} = \frac{\pi}{4} \cdot d_{CC}^2 \cdot (-z_{draft} - h_{BB}) \quad (11)$$

$$V_{RC,disp} = 3 \cdot \left( \frac{\pi}{4} \cdot d_{RC}^2 \right) \cdot (-z_{draft} - h_{BB}) \quad (12)$$

$$V_{BB,disp} = h_{bb} \cdot \left[ \frac{\sqrt{3}}{4} \cdot d_{RC}^2 + 3 \cdot \left( s_{radial} - d_{RC} \cdot \frac{\sqrt{3}}{4} \right) \cdot d_{RC} + 3 \cdot \left( \frac{\pi}{8} \cdot d_{RC}^2 \right) \right] \quad (13)$$

$$V_{disp} = V_{CC,sub} + V_{RC,sub} + V_{BB,sub} \quad (14)$$

where  $d_{CC}$  and  $d_{RC}$  are the center column and radial column diameters, respectively,  $z_{draft}$  is the draft of the foundation,  $h_{BB}$  is the bottom beam height, and  $s_{radial}$  is the radial spacing of the columns.

The mass of the water ballast for the installed system is calculated to match the input installed draft value. The equation to solve for the total water ballast mass in the system was derived and is given by Equation 15.

$$m_{WB} = \left[ \rho_{water} \cdot \frac{\pi}{4} \cdot (3 \cdot d_{RC}^2 + d_{CC}^2) \cdot (-z_{draft} - h_{BB}) + \rho_{water} \cdot V_{BB,sub} \right] - m_{fix,sys} \quad (15)$$

where  $m_{fix,sys}$  is the fixed mass of the total system. The total foundation mass is defined as the sum of the fixed mass of the foundation and the water ballast mass. The total system mass is defined as the sum of the total foundation mass, the RNA mass, and the tower mass.

The center of buoyancy (COB) can be calculated using the foundation volume geometry calculated above. The general equation to determine COB is given by Equation 16 and the equation for COB specific to the foundation geometry is given by Equation 17.

$$z_{COB} = \frac{\sum_i^n z_i V_i}{V_{total}} \quad (16)$$

$$z_{COB} = \frac{\frac{1}{2} \cdot (z_{draft} + h_{BB}) \cdot (V_{CC,disp} + V_{RC,disp}) + (z_{draft} + \frac{h_{BB}}{2}) \cdot V_{BB,disp}}{V_{disp}} \quad (17)$$

The water plane area is the area of the foundation hull at the waterline during installed draft. The water plane area of the foundation,  $A_{WP}$ , includes the cross-sectional area of the radial columns and center column. The area moment of inertia of the water plan area of the foundation is equivalent to the double integral of the water plane area. A general equation for moment of inertia is given in Equation 18 and the derived equation for the foundation water plane area moment of inertia is shown in Equation 19.

$$I_{y,WP} = \iint_A x^2 dA \quad (18)$$

$$I_{y,WP} = \frac{\pi}{4} \cdot \left\{ \left( \frac{d_{CC}}{2} \right)^4 + \left( \frac{d_{RC}}{2} \right)^4 + d_{RC}^2 \cdot s_{radial}^2 + 2 \cdot \left[ \left( \frac{d_{RC}}{2} \right)^4 + d_{RC}^2 \cdot (s_{radial} \cdot \sin 30^\circ)^2 \right] \right\} \quad (19)$$

The thickness of the steel for the floating foundation was calculated by dividing the hull steel mass by the product of the steel density and foundation surface area. The steel mass was determined through the mass scaling method used in Equation 9, using the steel mass value described in the VoltturnUS-S reference document. This provided an approximates of an increased steel thickness as the hull increases in size.

The mass of the bottom beam is determined by multiplying the surface area of the rectangular prism by the steel thickness and density. The center of gravity (COG) of the bottom beam in the x-direction is estimated as half of the radial spacing. The COG of the bottom beam in the z-direction is estimated using Equation 20.

$$z_{COG,BB} = z_{draft} + \frac{h_{bb}}{2} \quad (20)$$

The mass of the center and radial columns is determined using the same method as described for the bottom beam, using cylinders instead of a rectangular prism. The COG in the x-direction for the center column is zero and is the radial spacing value for the radial columns. The COG in the z-direction for all columns is estimated using Equation 21.

$$z_{COG,C} = z_{draft} + \frac{-z_{draft} + z_{freeboard}}{2} \quad (21)$$

The geometry of the water ballast within the foundation is first calculated by filling the volume of the three bottom beam legs with water until the desired mass is reached based on the density of ocean water. If the volume of water exceeds the volume of the bottom beams, then the volume of the three radial columns is filled from the bottom up until the desired mass is reached. The geometry of the concrete ballast is determined by filling the volume of the radial columns from the bottom up until the desired mass is reached, based on the density of the concrete.

The COG values for the water ballast in the bottom beam are calculated using the same method as the bottom beam COG values. The water ballast and concrete ballast in the radial columns is estimated to have a COG in the x-direction of the radial spacing value, and a COG in the z-direction based on the ballast heights in reference to the bottom of the column.

The COG for the turbine components in the x-direction was estimated as zero for the RNA and tower. The COG in the z-direction for the RNA was estimated as the hub height, and the ratio of COG to hub height from the baseline system was used to estimate the COG in the z-direction for the turbine tower.



The COG of the system was calculated using the COG values for each component of the system as outlined above. The equation for calculating COG in the z-direction of a multi-body system is shown in Equation 22.

$$z_{COG} = \frac{\sum_i^n z_i m_i}{m_{tot}} \quad (22)$$

where  $n$  is the number of bodies,  $i$  is the index value of the body,  $z_i$  is the COG of the body in the z-direction,  $m_i$  is the mass of the body, and  $m_{tot}$  is the total mass of the system.

The moment of inertia values for the system in the pitch direction (about the y-axis) are calculated within the model. The moment of inertia values for the center and radial column, as well as the turbine tower, are calculated using the equation for a walled cylindrical tube with open ends, shown in Equation 23.

$$I_{y,C,tower} = \frac{1}{12} \cdot m \cdot (3 \cdot (r_2^2 + r_1^2) + h^2) \quad (23)$$

where  $r_2$ , the outer radius of the cylinder, and  $r_1$ , the inner radius, are assumed to be close to equal for this application to simplify the equation.

The moment of inertia of the bottom beam was determined by calculating the moment of inertia of each rectangular plate that makes up the rectangular prism. The moment of inertia equations for the thin rectangular plates, with the axis of rotation going through the center in the normal direction and going through the center in the planar direction are given by Equation 24 and 25, respectively.

$$I_{y,BB,norm} = \frac{1}{12} \cdot m \cdot (a^2 + b^2) \quad (24)$$

$$I_{y,BB,plane} = \frac{1}{12} \cdot m \cdot a^2 \quad (25)$$

where  $a$  and  $b$  are appropriate side lengths of the rectangular plate.

The concrete and water ballasts in the radial columns, as well as the turbine rotor were modeled as disks, and the moment of inertia equation is shown in Equation 26.

$$I_{y,RCballast,rotor} = \frac{1}{4} \cdot m \cdot r^2 \quad (26)$$

The water ballast within the bottom beam is a solid rectangular prism, and the moment of inertia equation is given in Equation 27.

$$I_{y,BBballast} = \frac{1}{12} \cdot m \cdot (a^2 + b^2) \quad (27)$$

The nacelle was considered a point mass at the hub height of the turbine, and a point mass was added at the tower connection point on the foundation as described in the reference document. The moment of inertia contributions from a body in a multi-body system is calculated using Equation 28.

$$I_y = I_{Gy'} + m(x_G^2 + z_G^2) \quad (28)$$

where  $I_{Gy'}$  is the body's moment of inertia relative to its own COG,  $x_G$  is the COG of the body in the x-direction relative to the system COG, and  $z_G$  is the COG of the body in the z-direction relative to the system COG.

The total system moment of inertia about the y-axis was determined by first multiplying the sum of all the moment of inertia values from one leg of the foundation (radial column, bottom beam, ballasts) by 1.5 to account for the other two legs of the hull

located across the axis of rotation. The central moment of inertia values (center column and turbine components) were then added to find the total value for moment of inertia.

The added mass is the additional mass that is included in the system caused by the displacement of the water volume due to its motion. The added mass of the floating foundation was determined as outlined in Det Norske Veritas' (DNV) Recommended Practices in DNP-RP-C205 [25]. Appendix B contains the added mass coefficients from DNV. Pitch and heave are the main degrees of freedom of interest for this study, so the bottom beams created the only added mass to the system for this study. The columns have minimal influence on the added mass in heave, and for pitch at small angles the columns in this system can be estimated as moving in the heave direction. To account for some of the errors due to the added mass simplifications, the geometric length of the bottom beam was extended to include the extra length of the column radii.

The equation for added mass is shown in Equation 29.

$$m_A = \rho \cdot C_A \cdot A_R \quad (29)$$

where  $C_A$  is the added mass coefficient and  $A_R$  is the reference area; both values depend on geometry and lookup table values are provided in [DNV-RP-C205](#). The added mass was used to determine the added mass moment of inertia for the system.

The stiffness of the foundation in the pitch direction is given by Equation 30.

$$K_{\theta y} = \rho \cdot g \cdot I_{y,WP} + \rho \cdot g \cdot V_{disp} \cdot z_{COB} - m \cdot g \cdot z_{COG} \quad (30)$$

where  $\rho$  is the density of ocean water, and  $g$  is acceleration due to gravity.

The static pitch deflection, which is the angle at which the system will deflect during rated wind speeds, is calculated using Equation 31.

$$\theta_y = \frac{F_T L}{K_{\theta_y}} \quad (31)$$

where L is the moment arm, which is the distance between the hub height and the fairlead connection on the foundation.

The natural frequencies for the system in pitch and heave are given by Equations 32 and 33, respectively.

$$\omega_{n,pitch} = \sqrt{\frac{K_{\theta_y}}{I_y + I_{y,A}}} \quad (32)$$

$$\omega_{n,heave} = \sqrt{\frac{\rho g A_{WP}}{m + m_A}} \quad (33)$$

### Constraints

After completing the mathematical model in a MATLAB script, a range of turbine power sizes were selected for analysis. For each of the turbine sizes, the platform properties were tuned to achieve the minimum system mass while obeying certain constraints set to the systems. These constraints controlled the natural periods of the system, the geometric size of the platform, the pitch deflection of the platform at rated power, and the tow-out draft. The constraint values were selected based on accepted values for commercial systems and estimated acceptable size constraints for construction and transport of the platform. Table 1 shows the constraint values used in the model analysis in symbolic form.

Table 1. Symbolic model constraints

<b>System Property</b>	<b>Constraint Definition</b>
<b>Static Pitch Deflection</b>	$\theta_y < \theta_{\max,y}$
<b>Pitch Natural Period</b>	$T > T_{\min,\text{pitch}}$
<b>Heave Natural Period</b>	$T > T_{\min,\text{heave}}$
<b>Maximum Floater Width</b>	$w < w_{\max}$
<b>Minimum Bottom Beam Height</b>	$h_{\text{BB}} > h_{\text{BB},\min}$
<b>Tow-out Draft</b>	$d < d_{\text{towout},\max}$

### Initial Tuning

The initial tuning method was to change the radial spacing and radial column values manually until all the constraints were satisfied and the geometry resulted in approximately the minimum mass. The center column diameter was defined as equal to outer diameter of the turbine tower base, and the bottom beam height left at a constant value, equal to the value in the reference document. Once an approximate minimum mass design was achieved through manual inputs, a vector of values within a range of the original estimate was input into the model to achieve a finer tune of the minimum mass system. Once the final system design was determined by the model, all parameters of interest were recorded along with the tuned geometry specifications.

## RESULTS

### Problem Overview

The goal of the mathematical model was to observe trends of the floating offshore wind foundation as turbine power size increased. To that end, seven turbine power capacities were chosen for data collection. A base value of 15 MW would be a starting point to compare against the 15 MW VoltornUS-S, and then the power capacity would increase in 2.5 MW increments to 30 MW, making the turbine values as follows: 15 MW, 17.5 MW, 20 MW, 22.5 MW, 25 MW, 27.5 MW, and 30 MW. The mathematical model was developed using MATLAB [26] and the baseline code is given in Appendix C.

### Defining Constraints

A series of studies were conducted using different design constraints to determine how the constraints affect the key parameters of the offshore wind turbine foundation. The first study used basic constraint values determined by anticipated commercial parameters and estimated size limitations. This was used as a baseline as it generally followed the constraints outlined in the original VoltornUS-S design [19]. The second study increased the size constraint of the minimum foundation width, which was used to observe trends if construction techniques and port facilities were able to handle larger foundations. The third study had the same constraints as the baseline, but the size constraint on the bottom beam height was removed. Study three observed how the bottom beam height affected the foundation properties and represented a scenario where manufacturing techniques and materials may allow for smaller structural elements connecting the column structures in the foundation. The reasoning for the choice of

constraints is given in the Discussion section below. The values of the constraints for all three studies are shown in Table 2.

Table 2. Hull constraints

Hull Properties	Constraints		
	Study 1	Study 2	Study 3
<b>Static Pitch Deflection</b>	< 7 degrees	< 7 degrees	< 7 degrees
<b>Pitch Natural Period</b>	> 25 seconds	> 25 seconds	> 25 seconds
<b>Heave Natural Period</b>	> 18 seconds	> 18 seconds	> 18 seconds
<b>Maximum Floater Width</b>	< 100 meters	< 200 meters	< 100 meters
<b>Minimum Bottom Beam Height</b>	> 7 meters	> 7 meters	No Constraint
<b>Tow-out Draft</b>	< 10 meters	< 10 meters	< 10 meters

The static pitch deflection was determined by common design constraints for offshore wind turbines on floating hulls. The natural period constraints were chosen to avoid resonant motion with common wave spectrum periods. The baseline values for the maximum floater width and minimum bottom beam height for this study were based on the geometry of the VoltturnUS-S hull, which approximates expected port size limitations. The tow-out draft constraint was also based on expected values of semi-submersible hulls to meet port constraints.

#### Model Verification

The results of the mathematical model were compared against the values given in the VoltturnUS-S reference document to observe the accuracy of the mathematical calculations. The comparison between the reference values, the values obtained from the model using matching geometry, and the values obtained from the model based on the minimum mass using the constraints outlined in the first study is given in Table 3.

Table 3. Model comparison with reference

<b>System Property</b>	<b>VolturnUS-S Reference Values [19]</b>	<b>Model Values with Matching Geometry</b>	<b>Minimum Mass Model Values</b>
<b>Radial Column Diameter (m)</b>	12.50	12.50	12.70
<b>Radial Spacing (m)</b>	51.75	51.75	51.30
<b>Bottom Beam Height (m)</b>	7.00	7.00	7.00
<b>Total System Mass (Ballasted) (t)</b>	20093	20137	20406
<b>Hull Vertical Center of Buoyancy (SWL) (m)</b>	-13.63	-13.59	-13.55
<b>Hull Vertical Center of Buoyancy (SWL) (m)</b>	-14.94	-15.55	-15.78
<b>Pitch Natural Period (s)</b>	27.9	29.1	28.5
<b>Heave Natural Period (s)</b>	20.4	21.5	21.4

To quantify the accuracy of the data, the percentage error of the model values obtained using reference geometry was calculated relative to the reference values and given in Table 4.

Table 4. Percent error of model relative to VolturnUS-S reference

<b>System Property</b>	<b>Percent Error</b>
<b>Total System Mass (Ballasted)</b>	0.219%
<b>Hull Center of Buoyancy</b>	0.294%
<b>Hull Center of Gravity</b>	4.08%
<b>Pitch Natural Period</b>	4.76%
<b>Heave Natural Period</b>	5.19%



The quantified errors show a good correlation between the reference document and the model. The mass values are expected to be close due to the calculation of the fixed mass within the system based on the reference values, but the small errors do show that the calculation of the ballast mass based on the draft input and the model geometry is accurate. The small errors in the center of buoyancy and center of gravity calculations also show that the geometry in the model and the corresponding mass properties is accurate to the reference system. The natural period values were expected to have larger errors, due to the simplifications made in determining model geometry, mass, and added mass properties. The error only being ~5% for both natural period motions does provide some confidence in the model in determining the natural periods accurately enough to observe trends.

#### Platform Mass Trends

As described in the methodology section, the model calculated and recorded the foundation properties that corresponded to the minimum mass of the foundation that met the specified constraints. All foundation properties were defined by the system with the minimum calculated mass. The relationship between the minimum mass of the system and the turbine power for the three studies is plotted in Figure 4.

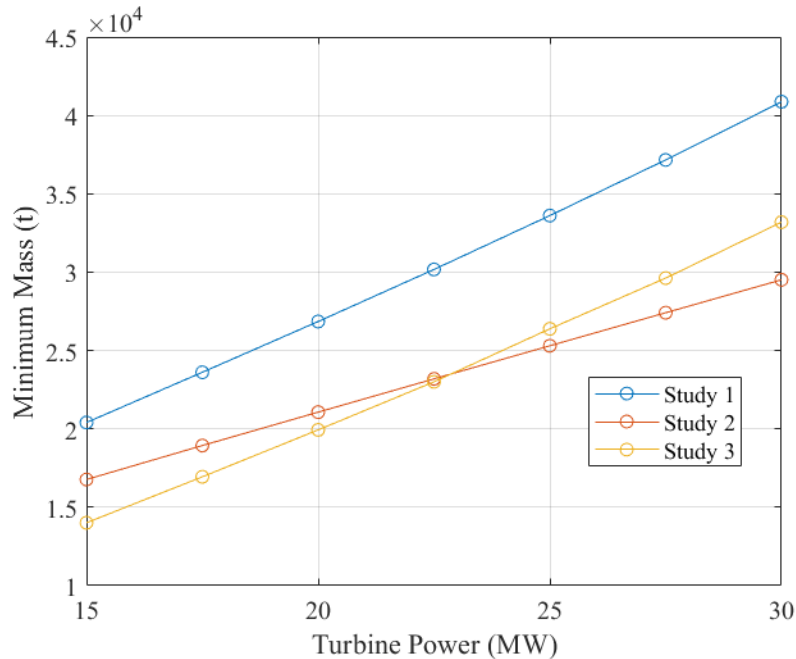


Figure 4. Minimum mass vs. turbine size

As turbine power increases, the minimum system mass increases in all three studies. The mass values were highest in study one for all turbine sizes. The minimum mass value of the entire data set occurred in study three at 15 MW turbine power, with a value of 14,011 metric tons. The minimum mass trend line for study three crossed with that of study two between 22.5 MW and 25 MW, meaning that for turbine sizes beyond the crossing point study two had the lowest mass values.

#### Platform Geometry Trends

The most critical foundation geometry in the studies conducted using the model were column properties, specifically the radial column diameter and the radial spacing between columns. The center column diameter was defined as equal to the turbine tower diameter, so the value was the same for all studies at each turbine size. The radial column diameter also defined the width of the bottom beam, making the value even more

important to the foundation properties. The column geometry that corresponded to the minimum foundation are plotted against the turbine power in Figure 5.

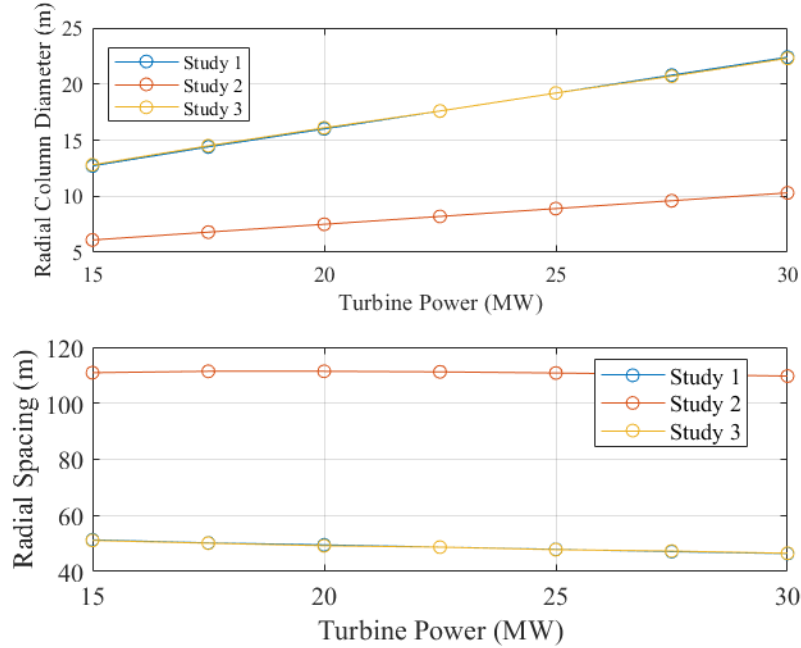


Figure 5. Radial column diameter and radial spacing vs. turbine size

The radial column diameter and column radial spacing were identical for the first and third studies, shown by the blue and yellow lines in the graph overlapping. For all studies, the radial column diameter increased linearly as turbine power increased. Radial spacing remained relatively constant for the foundations in all three studies, with a value of ~50m for the first and third studies, and ~110m for the second study. In the second study, the minimum mass corresponded to smaller radial column diameters and larger radial spacing of the columns.

The maximum width of the foundation was determined through geometric calculations defined by the radial column diameter and radial spacing values shown above. The maximum width is graphed against the turbine power rating in Figure 6.

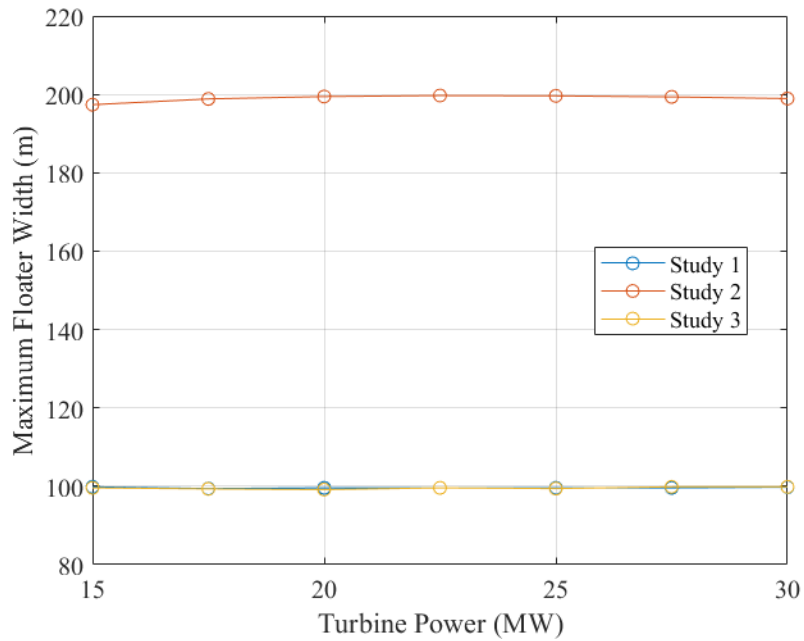


Figure 6. Maximum floater width vs. turbine size

For all three of the studies, the maximum floater width reached the upper limit constraint value for all turbine sizes. In studies one and three the width was ~100m, and in study two the width was ~200m. There is a slight variation in the values in the second study, with the width being slightly lower at 15 MW and 20 MW, but these variations are most likely due to the model search techniques rather than finding a true optimum value below the limit.

The bottom beam heights calculated in the three studies are given in Figure 7. The bottom beam height is the dimension in the z-direction of the bottom beam, relative to the bottom of the hull.

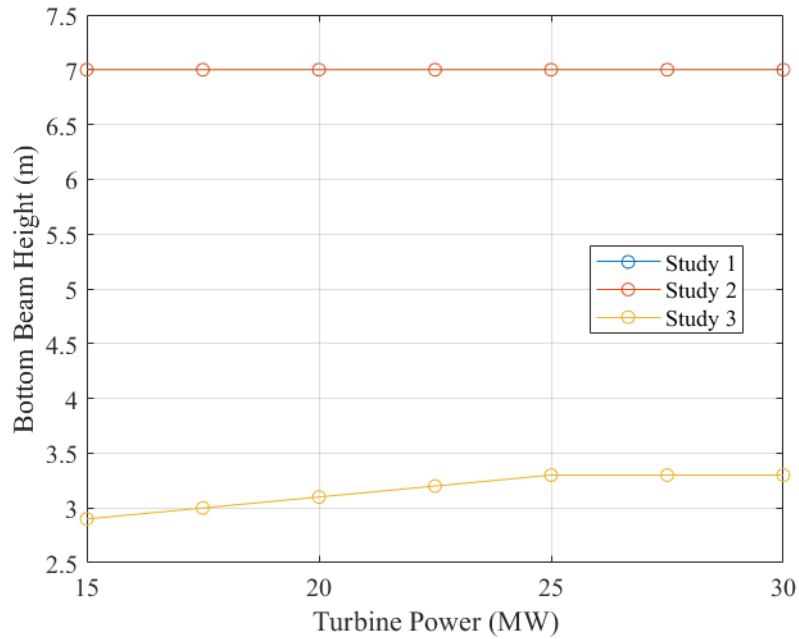


Figure 7 Bottom beam height vs turbine size

For study one and study two, the bottom beam height equaled the lower limit constraint of 7m for all turbine sizes. In the third study, with the bottom beam height unconstrained, the value at 15 MW was 2.9m, and rose in 0.1 steps to 3.3m at 25 MW. Above 25 MW, the bottom beam height remained constant at 3.3m.

### Constraint Trends

A key property of the floating offshore wind foundations is the natural frequencies and the corresponding periods of motion. The natural periods provide insight on the response of the system related to wind and wave loads. The natural periods of the foundations with the turbines installed are graphed against turbine power in Figure 8.

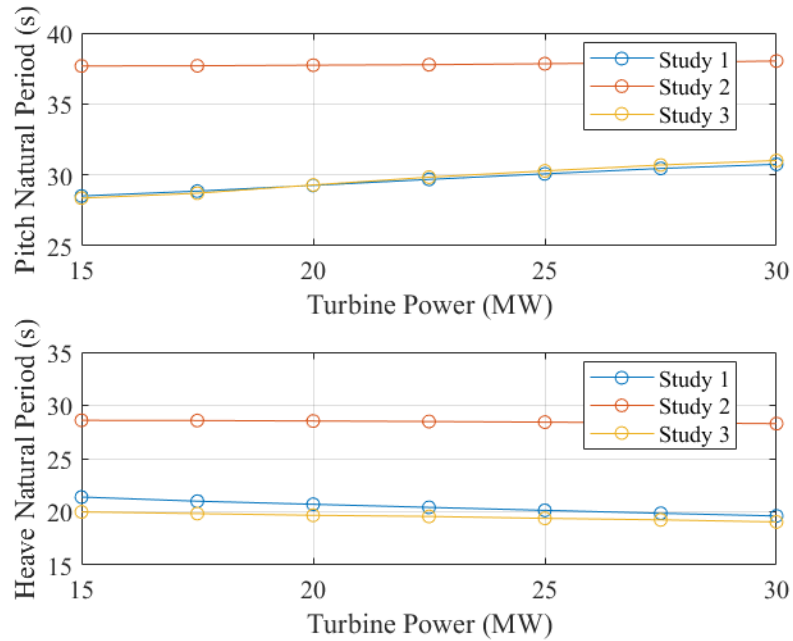


Figure 8. Pitch and heave natural periods vs. turbine size

Much like the column geometries, the natural periods of the system were similar between the first and third studies. For the two similar studies, the pitch natural period gradually increased linearly as turbine power increased, trending further away from the 25 second lower limit. For the same two studies, the heave natural period gradually decreased linearly, approaching closer to the 18 second lower limit as turbine size increased. For the second study, the natural periods were greater than those in the other studies, and the periods remained relatively constant as turbine power increased, with periods of ~38 seconds for pitch and ~28 seconds for heave.

The static pitch deflection due to the scaled thrust loads are plotted against the turbine power in Figure 9. The deflection values represent the pitch angle of the foundations at rated wind speed, when thrust loads are highest.

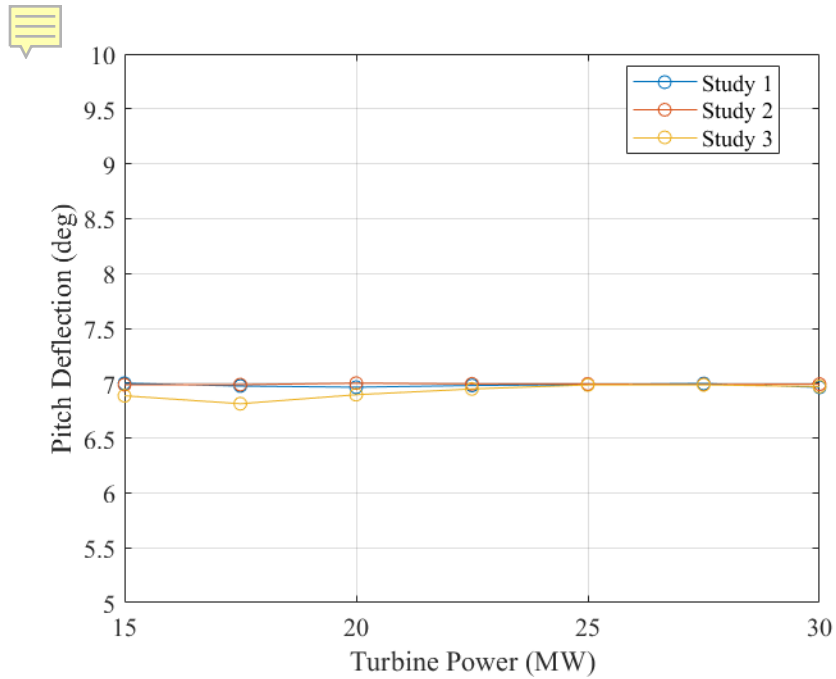


Figure 9. Pitch deflection vs. turbine size

The pitch deflections for all three studies were essentially against the upper limit of 7 degrees for all turbine sizes. The trends from the data show that the minimum mass systems produced the largest pitch deflections, so the model search resulted in maximum allowable values.

Another key geometric feature of foundation is the tow-out draft, defined in this study as the draft with the turbine installed and with no water ballast. The tow-out draft of the foundation with the turbine installed is graphed against the turbine power in Figure 10.

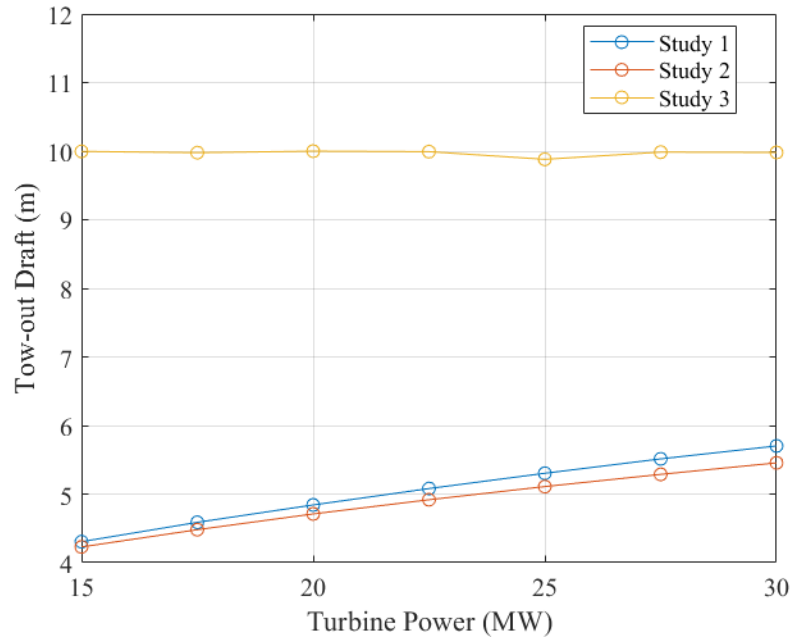


Figure 10. Tow-out draft vs. turbine size

For studies one and two, the tow-out draft increased linearly, from ~4m to ~6m, as turbine power increased. The tow-out draft for study one was slightly higher than that in study two for all turbine sizes. In the third study, the tow-out draft increased considerably to reach a constant value of ~10m for all turbine sizes, which was the upper limit of tow-out draft as defined in the constraints.

#### Relative Cost

To compare the relative costs of the three studies, the minimum mass was divided by the turbine power rating at each point, resulting in a mass per megawatt value that was graphed against the turbine power in Figure 11.



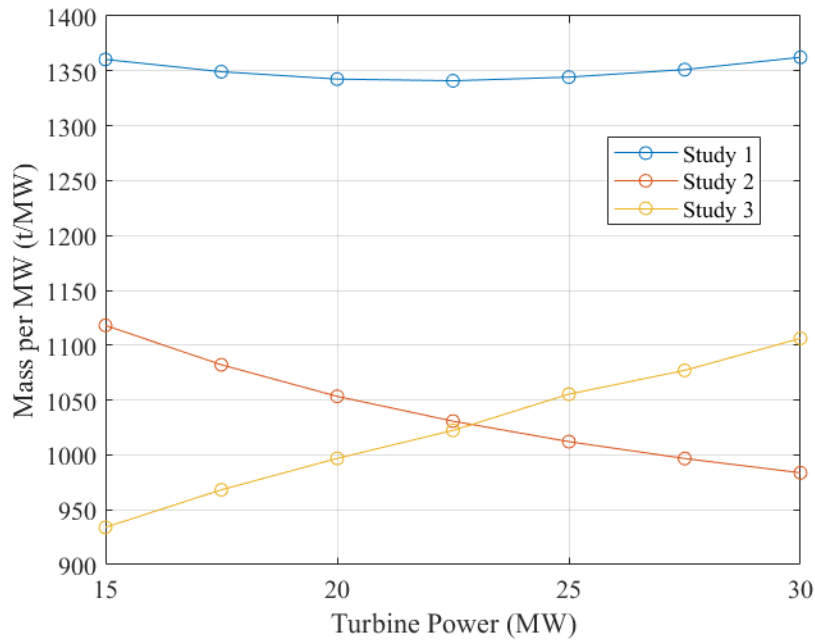


Figure 11. Mass per megawatt vs. turbine size

The baseline constraints in the first study had the largest mass per megawatt, with a value of  $\sim 1350$  t/MW for all turbine sizes. The curve for study one was slightly parabolic in shape, having a minimum value between 20 MW and 22.5 MW.

In study two, the increased limit on foundation width allowed the mass per megawatt to decrease significantly compared to the baseline. The mass per megawatt started out at a value of 1118 t/MW at 15 MW turbine size and decreased as turbine size increased. The effect of the changed constraints in the third study had the opposite trend. In study three the mass per megawatt was also significantly lower than the baseline values, and at 15 MW turbine size the mass per megawatt was the lowest value across the entire experiment, with a value around 934 t/MW. As turbine sizes increased in study three, the mass per megawatt increased, crossing with the line of study two between 22.5 MW and 25 MW.

## DISCUSSION

### Study One: Baseline Constraints

The values obtained by the model using the methodology and constraints outlined in study one provides different geometry that has a higher mass value than both the reference and the values obtained from using the reference geometry in the model. The differences are due to two reasons, the model used a step size of 0.1m between geometry values, so a radial spacing value of 51.75m was not used in calculations, and the reference geometry results in a maximum hull width of 100.46m, which means it did not meet the constraints of the study. Although the mathematical model's minimum mass was higher than the reference design, it was determined that the model was within a reasonable margin to achieve the goals of the study.

Based on the mass per megawatt data, the value for the hulls within the first study was relatively constant. The mass per megawatt did reach a minimum at 20 MW, but this value was only a 1.82% difference from the maximum mass per megawatt value at 30 MW. With mass being assumed as a relative proxy of cost, there appears to be no change to costs directly related to the hull by upscaling the turbine if the constraints from the first study are applicable. Using larger turbines does offer the advantage of constructing, installing, operating, and decommissioning less hulls to achieve the same amount of total power capacity in a floating offshore wind farm setting. Based on the data, these advantages would come at relatively no additional cost to the mass per megawatt between 15 MW and 30 MW.

To investigate the causes of the mass per megawatt trend in the first study, the constrained parameters were observed to understand what changes may allow the hull mass to decrease. The key parameters limited by the constraints were maximum hull width, bottom beam height, and the pitch deflection under maximum thrust loads. The pitch deflection constraint is largely determined by the turbine operational limits, so the hull geometric constraints were chosen to explore further.

For all turbine sizes in the first study, the maximum hull width was above 99m, within 1% of the 100m upper limit. The hull width is defined by the relationship between the radial column diameter and radial column spacing. As the turbine size increased in the first study, the need for increased size of the hull to meet the constraints was done by increasing the diameter of the radial columns and decreasing the radial spacing, which allowed the maximum width to remain relatively constant just below the 100m limit.

#### Study Two: Expanded Hull Maximum Width

The findings from the first study prompted the change in the maximum allowable hull width in study two. The increase in the constraint on maximum hull width from 100m to 200m was a relatively arbitrary change in size, but it allowed for a large enough increase to observe trends in the hull properties. Leaving the maximum hull width unconstrained resulted in unusable data, so the 200m value was chosen. Increasing the maximum width constraint to 200m allowed the hull to decrease in mass. The percentage decrease of the total system mass calculated in study two relative to the values in study one for each turbine size is given in Table 5.

Table 5. Study two: percent decrease in mass relative to study one

<b>Turbine Size</b>	<b>Percent Decrease in Mass</b>
<b>15</b>	18.2
<b>17.5</b>	19.8
<b>20</b>	21.1
<b>22.5</b>	22.9
<b>25</b>	24.5
<b>27.5</b>	26.0
<b>30</b>	27.4

The decrease in mass relative to the study one values increased as turbine size increased. The mass per megawatt decreased as turbine size increased, making it more cost effective to design larger turbines with the greater maximum width constraint. The data collected in study two suggests that a larger hull width produces more mass-efficient and cost-efficient hulls.

As the demand for larger turbines increases, it appears that the ideal floating hulls would include long, slim members, and smaller diameter columns. For all turbine sizes, the radial column diameters of the second study were less than half the original diameters in study one and the radial spacing approximately doubled. The long and slim members also achieved greater natural period responses as compared to the first study, suggesting that the wider hulls would be more stable in the water.

#### Study Three: Bottom Beam Height Constraint Removed

The bottom beam length was constant at the lower limit of 7m for all turbine sizes in both the first and second study, indicating that any increase in the bottom beam height above the constraint added unneeded extra mass. To achieve a smaller mass value, the bottom beam height constraint was completely removed for the third study, with all other constraints remaining the same as study one.

The column geometry corresponding to the minimum hull masses in the third study was the same as the values in the first study, meaning the hull width values were also the same. Achieving the same geometry between the two studies indicates that for this model, bottom beam height did not influence the column geometry corresponding to the minimum hull mass for all turbine sizes. Instead, the maximum width constraint is what determined the radial column diameters and the radial spacings. The natural periods in both pitch and heave motion were also similar between study one and study three, indicating that the column geometry determined the natural periods of the systems in this model, while changing the bottom beam height had little effect.

The removal of the bottom beam height constraint in the third study resulted in lower calculated minimum system mass as compared to the values in study one. The percentage decrease in mass for the systems in study three relative to study one is given in Table 6.

*Table 6. Study three: percent decrease in mass relative to study one*

<b>Turbine Size</b>	<b>Percent Decrease in Mass</b>
<b>15</b>	31.5
<b>17.5</b>	28.4
<b>20</b>	25.9
<b>22.5</b>	23.6
<b>25</b>	22.0
<b>27.5</b>	20.4
<b>30</b>	18.8

In the third study the mass was lower for all turbine sizes relative to the values in study one. The low-profile bottom beam is more cost-efficient than the original size constraints, indicating that smaller structural members between columns may be beneficial to hull design at this scale. There are other semi-submersible hulls, such as the

OC4-DeepCwind shown in Figure 12, that use relatively small tubular members to connect the columns together, as opposed to the rectangular bottom beam structure of the VoltturnUS-S design.

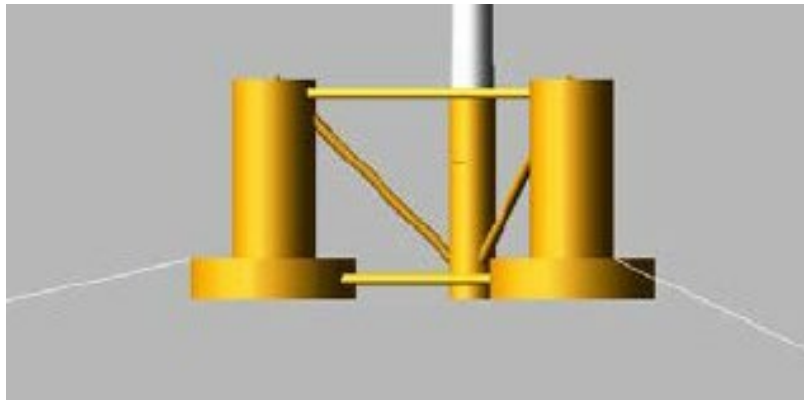


*Figure 12. OC4-DeepCwind semi-submersible hull*

*Source: Adapted from [22]*

Interestingly, the mass per megawatt increased as turbine size increased, meaning smaller turbines are more cost-efficient compared to larger ones when the bottom beam has no constraint. The most cost-efficient system in all three studies was the hull with the 15 MW turbine in study three, with an unconstrained bottom beam height. As the turbine size increased in study three, the percent decrease in mass relative to the first study decreased, which was the opposite trend as that seen in the second study.

A significant feature of the data in the third study was the change in the tow-out draft of the system as compared to the other two studies. In the first two studies, the tow-out draft was well below the 10m upper limit, increasing gradually between 4m and 6m as turbine size increased. In study three, the tow-out draft jumped up to the upper limit value for all turbine sizes. The constant value indicates that the tow-out draft was the limiting parameter on the bottom beam height, not allowing it to decrease further. The

tow-out draft is dependent on the buoyancy provided by the structure, so the bottom beam height was decreasing the value that correlated to the minimum bottom beam volume that provided the buoyancy needed for the tow-out draft constraint.

### Comparison of Studies

For both the second and third studies, the mass of the system at all turbines sizes was lower than the masses observed in the first study. Study three results contained the lowest mass systems at the lower turbine values, starting at 15 MW, until 22.5 MW where the second study reached a similar mass value as that in the third study. As turbine size increased past 22.5 MW, the study two resulted in the lowest mass systems. The crossing point between the two studies indicates that when attempting to achieve the lowest mass hull, different parameters are more efficient in reducing mass depending on the turbine size. At turbine sizes below 22.5 MW, it is more effective to reduce the bottom beam height, aiming for lower-profile structural members between the columns of the semi-submersible hull. For turbines above 22.5 MW, increasing the maximum width of the hull, allowing for longer and slimmer members with smaller diameter columns, is more effective in reducing the mass of the system.

### Limitations

The limitations in the methodology of creating the mathematical model result in questions over the significance of the hull designs produced. The structural properties and mechanics of the hull are not explored beyond their geometry. As features of the system increased in size, such as column radii, the bottom beam, and the turbine assembly, the mass of these features also increased which results in increased loads throughout the structure. Notably, in the second study, the longer radial spacing results in a larger

moment on the structure where the leg member of the hull connects to the center of the structure. The reduced radial column diameters, and resulting smaller bottom beam width, caused greater stresses in the structure due to a smaller section modulus. Similarly, the reduced bottom beam height in the third study also results in smaller cross-sectional areas in the bottom beam members, decreasing the section modulus and increasing the stresses within the structure.

A further exploration in the structural mechanics of the hull properties generated by the mathematical model may prove that they are not viable designs. The hulls may require additional structural reinforcement and alterations to geometry, such as increased steel thickness, that would change the mass of the system considerably. Although the designs lack an analysis of structural mechanics, they are still valuable in observing trends of system parameters dependent on the mass and geometry, aiding in future design choices.

The effect of mooring lines on the system was omitted from the calculations of the mathematical model. The model was simplified due to the relatively small effect that catenary moorings have on the motion of semi-submersible hulls in the degrees of freedom examined in this research. The natural periods of the system calculated in the model, in both pitch and heave motions, would be affected by mooring lines in some capacity. The costs associated with mooring lines may also increase as the hull size increases, as larger, stronger, and a greater number of mooring lines may be required.

There are an extensive number of factors that go into the cost-efficiency of a FOWT system. To simplify the comparison of the hulls, the mass of the system was used to estimate the relative cost. It is important to consider the effects that increasing turbine



and hull size has during construction, assembly, transportation, installation, operation, maintenance, and decommissioning that all influence the costs associated with the turbine. Exploring the other factors would take extensive time and resources, but it is necessary to design a viable FOWT system.

The constraints put on the system in each of the studies described above put limitations on the relevancy of the results. The constraints were mainly chosen to clearly show trends from a big-picture perspective, generally based on the values described for the VoltturnUS-S system. In reality, the constraints placed on a FOWT system are site-dependent and unique for every project. Properties of the port and transportation route would determine the maximum width and tow-out draft constraints, which are influential parameters to the results in all three studies described above.

## CONCLUSION

### Findings

A mathematical model based on hydrostatic properties was developed to analyze the effects and trends of upscaling the turbine size for FOWT systems. The UMaine VolturnUS-S floating semi-submersible, designed to support the IEA-15MW turbine was chosen as the baseline design in determining the mass and geometric properties of the system calculated in the model. A simple comparison of the model results to the values provided in the reference document showed that there was a reasonable amount of mathematical accuracy to generate significant data used to inform observations.

Three studies were conducted using the model, exploring how changing constraints on system properties affected the resulting parameters. The first study set baseline parameters based on the VolturnUS-S system and common design characteristics of semi-submersible foundations used for FOWT. The results from the first study showed that the mass of the system increased as turbine size increased, but that the mass per megawatt remained relatively constant for each turbine size observed. The second point suggested that the relative cost of the turbine per megawatt did not change as turbine size increased. The data from the first study also revealed that the radial spacing and the bottom beam height were two geometric constraints limiting the results, which informed the constraint changes in the next two studies.

The second study increased the constraint on the maximum hull width from 100m to 200m. The results showed that the hull mass significantly decreased as compared to the results from the first study due to geometry changes allowed by the increased width. The radial column diameters decreased, while the radial spacing increased, creating long,

thin members connecting the radial columns to the center. The mass per megawatt of the systems generated in study two decreased as turbine size increased, suggesting that the cost-efficiency of the turbine system increased as the turbine size increased.

The third study removed the constraint on the bottom beam height of the hull. The mass of the hulls also significantly decreased when compared to the results of the first study. The bottom beam heights decreased until the buoyancy of the hull decreased to a point where the tow-out draft limit was reached. The decrease in mass suggested that decreasing the size of the structural members that connected the columns of the hull had a positive effect on cost efficiency. The column geometry and the natural period motions of the system were like the values in study one, indicating that these parameters were not influenced heavily by bottom beam height. The mass per megawatt of the systems generated in study three increased as turbine size increased, suggesting that the cost-efficiency decreased as turbine size increased.

A comparison of the result from study two and study three revealed interesting trends related to floating hull design. When observing the mass per megawatt of the two studies, the systems generated by study three were the lowest from 15 MW to 22.5 MW. At 22.5 MW the result of study two reached a similar value creating a crossing point, where above 22.5 MW the systems generated by study two resulted in the lowest value. The results suggest that below 22.5 MW, creating low-profile and smaller structural members between the columns is the most cost-effective way of reducing mass, while above 22.5 MW, designing hulls with larger maximum widths is most effective.

### Research Significance and Contributions

The results of this research provide insight into trends of FOWT hulls as turbine size increases. Turbine power capacities are currently increasing at a high rate, and hull designs need to keep up for the technology to be viable for the future. Creating a model to explore trends in upscaling from a big-picture prospective can provide insight into more detailed design directions for the future. The model described above provides a relative starting point to determine the properties of a FOWT system given a turbine size. Additional time and resources would be required to reach a viable and optimized design, but the model described above provides the preliminary design trends that may be of interest.

### Future Research

Floating offshore wind is an extensive area of research that is evolving at an increasingly rapid pace to address the future need for clean energy. The methodology and model described above is simply a piece of the puzzle that goes into the analysis of FOWT design. Developing the mathematical model to include an analysis of the structural mechanics of the hull would provide valuable insight into the viability of certain hull designs, and what effect the properties have on the mechanics of the system. Mooring line analysis could be added to the model to allow for more detailed and accurate calculation of the system motions. A more detailed cost analysis could factor in the aspects of construction, installation, and marine operations that may be influenced by the size of the system. The additions and improvements that could be made to this research are limitless, representing the complexity and opportunity of offshore floating wind for the future.

## BIBLIOGRAPHY

- [1] W. Musial, P. Spitsen, P. Duffy, P. Beiter, M. Marquis, R. Hammond, and M. Shields, “Offshore wind market report: 2022 edition,” 2022.
- [2] H. Díaz and C. Guedes Soares, “Review of the current status, technology and future trends of offshore wind farms,” *Ocean Engineering*, vol. 209, 2020. 10.1016/j.oceaneng.2020.107381.
- [3] “Infographic: Offshore Wind in Maine”, *The University of Maine*. 2016. [Online]. Available: [https://composites.umaine.edu/wp-content/uploads/sites/20/2016/12/UMaineCompositesCenter\\_OffshoreWind\\_12122016.pdf](https://composites.umaine.edu/wp-content/uploads/sites/20/2016/12/UMaineCompositesCenter_OffshoreWind_12122016.pdf)
- [4] “Fact sheet: Biden-Harris Administration announces new actions to expand U.S. Offshore Wind Energy,” *The White House*. 2022. [Online]. Available: <https://www.whitehouse.gov/briefing-room/statements-releases/2022/09/15/fact-sheet-biden-harris-administration-announces-new-actions-to-expand-u-s-offshore-wind-energy/>
- [5] H. Díaz, J. Serna, J. Nieto, and C. Guedes Soares, “Market needs, opportunities and barriers for the floating wind industry,” *Journal of Marine Science and Engineering*, vol. 10, no.7, p. 934, 2022.
- [6] R. Wiser, J. Rand, J. Seel, P. Beiter, E. Baker, E. Lantz, and P. Gilman, “Expert elicitation survey predicts 37% to 49% declines in wind energy costs by 2050,” *Nature Energy*, vol.6, no. 5, pp. 555–565, 2021.
- [7] D. Matha, C. Brons-Illig, A. Mitzlaff, and R. Scheffler, “Fabrication and installation constraints for floating wind and implications on current infrastructure and design,” *Energy Procedia*, vol. 137, pp. 299-306, 2017.
- [8] M. Shields, R. Marsh, J. Stefek, F. Oteri, R. Gould, N. Rouxel, K. Diaz, J. Molinero, A. Moser, C. Malvik, and S. Tirone, “The Demand for a Domestic Offshore Wind Energy Supply Chain,” *Golden, CO: National Renewable Energy Laboratory*. NREL/TP-5000-81602. 2022. [Online]. Available: <https://www.nrel.gov/docs/fy22osti/81602.pdf>
- [9] M. Leimeister, E. E. Bachynski, M. Muskulus, and P. Thomas, “Rational upscaling of a semi-submersible floating platform supporting a wind turbine,” *Energy Procedia*, vol. 94, pp. 434–442, 2016.
- [10] K. L. Dykes, J. Rinker, “Windpact reference wind turbines”, Technical Report, National Renewable Energy Lab. (NREL), Golden, CO (United States), 2018.
- [11] M. Saeki, I. Tobinaga, J. Sugino, T. Shiraishi, “Development of 5-MW offshore wind turbine and 2-MW floating offshore wind turbine technology”, *Hitachi Review*, vol. 63, p. 414, 2014.
- [12] J. Jonkman, S. Butterfield, W. Musial, G. Scott, “Definition of a 5-MW reference wind turbine for offshore system development”, Technical Report, National Renewable Energy Lab. (NREL), Golden, CO (United States), 2009.

- [13] C. Desmond, J. Murphy, L. Blonk, W. Haans, “Description of an 8 MW reference wind turbine”, *Journal of Physics: Conference Series*, vol. 753, p. 092013, 2016.
- [14] C. Bak, F. Zahle, R. Bitsche, T. Kim, A. Yde, L. C. Henriksen, M. H. Hansen, J. P. A. A. Blasques, M. Gaunaa, A. Natarajan, “The DTU 10-MW reference wind turbine”, *Danish Wind Power Research*, 2013.
- [15] P. Bortolotti, H. Canet Tarrés, K. Dykes, K. Merz, L. Sethuraman, D. Verelst, F. Zahle, “Systems engineering in wind energy-WP2”, Technical Report, Technical Report No. NREL/TP-5000-73492, National Renewable Energy, 2019.
- [16] C. E. Silva de Souza, P. A. Berthelsen, L. Eliassen, E. E. Bachynski, E. Engebretsen, H. Haslum, “Definition of the INO WINDMOOR 12 MW base case floating wind turbine”, Technical Report, SINTEF Ocean, 2021.
- [17] E. Gaertner, J. Rinker, L. Sethuraman, F. Zahle, B. Anderson, G. Barter, N. Abbas, F. Meng, P. Bortolotti, W. Skrzypinski, et al., “Definition of the IEA 15-Megawatt offshore reference wind turbine”, Technical Report, National Renewable Energy Lab. (NREL), Golden, CO (United States), 2020.
- [18] T. Ashuri, J. R. Martins, M. B. Zaaijer, G. A. van Kuik, G. J. van Bussel, “Aeroservoelastic design definition of a 20 MW common research wind turbine model”, *Wind Energy*, vol. 19, pp. 2071–2087, 2016.
- [19] C. Allen, A. Viselli, H. Dagher, A. Goupee, E. Gaertner, N. Abbas, M. Hall, and G. Barter. “Definition of the UMaine VoltturnUS-S Reference Platform Developed for the IEA Wind 15-Megawatt Offshore Reference Wind Turbine,” *Golden, CO: National Renewable Energy Laboratory*. NREL/TP-5000-76773. [Online]. Available: <https://www.nrel.gov/docs/fy20osti/76773.pdf>
- [20] J. V. Taboada, "Comparative analysis review on floating offshore wind foundations (FOWF)." *Proceedings of the 54th Naval Engineering and Maritime Industry Congress*, Ferrol, Spain. 2015.
- [21] J. Z. Wu, "A Method to Upscale a Floating Offshore Wind Turbine from 5 MW to 15 MW." Master of Science Thesis, Ocean Engineering, Texas A&M University, 2021.
- [22] A. Roberson, J. Jonkman, M. Masciola, H. Song, A. Goupee, A. Coulling, C. Luan, “Definition of the Semisubmersible Floating System for Phase II of OC4”, Technical Report, National Renewable Energy Lab. (NREL), Golden, CO (United States), 2014.
- [23] N. Y. Sergiienko, L. S. P. da Silva, E. E. Bachynski-Polić, B. S. Cazzolato, M. Arjomandi, and B. Ding, “Review of scaling laws applied to floating offshore wind turbines,” *Renewable and Sustainable Energy Reviews*, vol. 162, p. 112477, 2022.
- [24] K. A. Stol, “Dynamics modeling and periodic control of horizontal-axis wind turbines”, Ph.D. Thesis, Department of Aerospace Engineering Sciences, University of Colorado, 2001.
- [25] *DNV Recommended Practice for Environmental Conditions and Environmental Loads*, DNV-RP-C205, 2010

[26] The MathWorks, Inc. (2022). MATLAB version: 9.13.0 (R2022b). [Online]. Available: <https://www.mathworks.com>.

## APPENDICES



APPENDIX A

SERGIENKO ET. AL. TURBINE SCALING EQUATIONS [23]

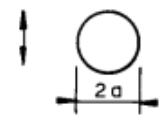
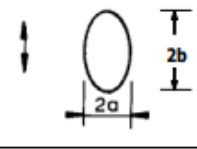
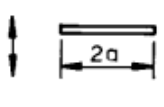
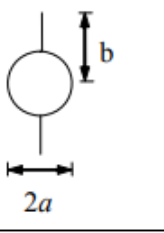
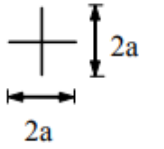
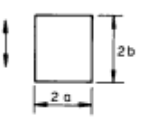
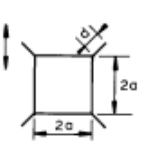
Parameters for the reference (not commercial) offshore wind turbines and associated tower designs for both fixed-bottom and floating support structures. All the values have been taken from the corresponding references provided in the table. The scaling laws have been identified by the authors based on the data in the table. The scaling laws include: (i) best power fit as  $y = aD^b$ , where  $D$  is the rotor diameter, and coefficients  $a$  and  $b$  are unknown, and (ii) heuristic engineering approach as  $y = cD^d + f$ , where  $c$  and  $f$  are unknown ( $f \neq 0$  for the tower linear dimensions), and the exponent  $d$  is maintained constant according to the expected geometric upscaling.

Wind turbine	Scaling law									
	Best power fit (R <sup>2</sup> )	Heuristic engineering fit (R <sup>2</sup> )	1.5 MW	2 MW	5 MW	8 MW	10 MW	12 MW	15 MW	20 MW
Rated power, MW	$821D^{1.79}$ (99.1%)	$267D^2$ (98.5%)	1.5	2	5	8	10	12	15	20
Rotor diameter, m	$D$	$D$	70	80	126	164	178.3	198	240	276
Rated wind speed, m/s			11.4	12	11.4	12.5	11.4	11	10.6	10.7
Tip speed, m/s			75	73.3	80	6.3	90	88.6	95	103.3
Rotor speed min, rpm	$245D^{-0.71}$ (96.2%)	$982D^{-1}$ (78.5%)		11.1	6.9	6.3	6	6	5	4.5
Rotor speed max, rpm	$731D^{-0.84}$ (99.1%)	$1561D^{-1}$ (95.5%)	20.5	19.6	12.1	10.5	9.6	8.7	7.6	7.1
Drive/gearbox ratio			88:1	98:1	97:1	N/A	50:1	Direct	Direct	164:1
Peak thrust, kN	$84D^{1.86}$ (97.3%)	$40.3D^2$ (97.1%)	250	300	700	1050	1500	1350	1950	2300
Blade mass, t	$3.07D^{1.83}$ (98.7%)	$1.19D^2$ (98.2%)	4.3	6.9	17.7	35	41.7	47.7	65	86.3
Hub mass, t	$0.23D^{2.46}$ (83.0%)	$2.89D^2$ (81.6%)	19.2	20.2	56.8	90	105.5	81.7	190	252.8
Rotor mass, t	$5D^{2.05}$ (97.2%)	$6.46D^2$ (97.2%)	32.2	41.2	110	195	230	225	385	511.8
Nacelle mass, t	$24.3D^{1.88}$ (97.6%)	$12.3D^2$ (97.4%)	52.8	75.2	240	285	446	543	630	945
Tower mass, t										
- fixed-bottom	$12.65D^{2.07}$ (93.5%)	$18.63D^2$ (93.5%)	125.4	196.5	347.5	558	605	628	860	1588.3
- floating*					249.7*		1257*	1162*	1263*	
Tower height, m	$3.41D^{0.67}$ (86.8%)	$0.43D^1 + 30$ (86.9%)	82.4	75.8	87.6	106.3	115.6	115.6	129.6	155
Hub height, m	$2.41D^{0.75}$ (97.5%)	$0.47D^1 + 31$ (97.6%)	84	80	90	110	119	119	150	160
Tower diameter (bottom), m	$0.23D^{0.68}$ (94.5%)	$0.032D^1 + 2.23$ (92.7%)	5.66	4.3	6	7.7	8.3	8.3	10	10
Tower diameter (top), m	$0.15D^{0.68}$ (92.4%)	$0.020D^1 + 1.39$ (89.5%)	2.57	2.5	3.87	5	5.5	5.5	6.5	6.2
Tower thickness (bottom), mm										
- fixed-bottom	$0.16D^{1.06}$ (97.3%)	$0.22D^1$ (96.8%)	17.39	32	27	36	38	38	N/A	63
- floating*							75*	90*	83*	
Tower thickness (top), mm										
- fixed-bottom	$0.18D^{0.93}$ (79.1%)	$0.12D^1$ (78.8%)	10.26	18	20	22	20	20	N/A	39
- floating*							29*	30*	21*	
Tower natural frequency, Hz										
- fixed-bottom	$26.4D^{-0.91}$ (95.7%)	$42.94D^{-1}$ (94.7%)		0.3328	0.324		0.25	0.24	0.17	0.1561
- floating*					0.42*		0.55*	0.641*	0.496*	

APPENDIX B

DNV-RP-C205 ADDED MASS COEFFICIENTS [25]

**Table D-1 Analytical added mass coefficient for two-dimensional bodies, i.e. long cylinders in infinite fluid (far from boundaries). Added mass (per unit length) is  $m_A = \rho C_A A_R$  [kg/m] where  $A_R$  [m<sup>2</sup>] is the reference area.**

Section through body	Direction of motion	$C_A$	$A_R$	Added mass moment of inertia [(kg/m) × m <sup>2</sup> ]		
		1.0	$\pi a^2$	0		
	Vertical	1.0	$\pi a^2$	$\rho \frac{\pi}{8} (b^2 - a^2)^2$		
	Horizontal	1.0	$\pi b^2$			
	Vertical	1.0	$\pi a^2$	$\rho \frac{\pi}{8} a^4$		
	Vertical	1.0	$\pi a^2$	$\rho a^4 (\csc^4 \alpha f(\alpha) - \pi^2) / 2\pi$ where $f(\alpha) = 2\alpha^2 - \alpha \sin 4\alpha$ $+ 0.5 \sin^2 2\alpha$ and $\sin \alpha = 2ab / (a^2 + b^2)$ $\pi/2 < \alpha < \pi$		
	Horizontal	$1 - \left(\frac{a}{b}\right)^2 + \left(\frac{a}{b}\right)^4$	$\pi b^2$			
	Horizontal or Vertical	1.0	$\pi a^2$	$\frac{2}{\pi} \rho a^4$		
	Vertical	1.0	$\pi a^2$	$\beta_1 \rho \pi a^4$ or $\beta_2 \rho \pi b^4$		
				$a/b$	$\beta_1$	$\beta_2$
				0.1	-	0.147
				0.2	-	0.15
				0.5	-	0.15
				1.0	0.234	0.234
				2.0	0.15	-
				5.0	0.15	-
				$\infty$	0.125	-
	Vertical	1.61 1.72 2.19	$\pi a^2$	$\beta \rho \pi a^4$		
				$d/a$	$\beta$	
				0.05 0.10 0.10	0.31 0.40 0.69	

APPENDIX C  
MATHEMATICAL MODEL MATLAB CODE

```
%% User Inputs

% Input Turbine Power (MW)

power_MW_range = [15 17.5 20 22.5 25 27.5 30] ;

for q = 1:length(power_MW_range)
    power_MW = power_MW_range(q)

% Input Installed System Draft (m)

install_draft = 20 ;

% Hull Geometry Tuning (m)

rc_d_i = (10:0.1:30) ;
radial_spacing_i = (30:0.1:55) ;

bb_h_i = (7:0.1:8) ;
freeboard = 15;
fairlead = -14;

[rc_d,radial_spacing,bb_h] = meshgrid(rc_d_i,radial_spacing_i,bb_h_i);

%% Calculations

% Constants

ocean_rho = 1025;    % (kg./m^3)
g = 9.81;           % (m./s^2)

% Rotor Diameter (m)

rotor_d = (power_MW.*1e6./821)^(1./1.79);
tower_d = 0.23*rotor_d^0.68;

cc_d = tower_d ;

% Geometry

bb_l = radial_spacing-cc_d./2-rc_d./2;
bb_l_ext = radial_spacing+rc_d./2;

% Scale Factors

s = rotor_d./240;
p_xy = s;
p_z = 1;
Rd = 1.63.*rotor_d^1.09;
```

```

% Water Plane Area (m^2) (BB submerged)

waterplane_a = pi./4.*(3.*rc_d.^2+cc_d.^2);

% Displaced Volume Calculations (m^3)

bb_v = bb_h.*(sqrt(3)./4.*rc_d.^2+3.*(radial_spacing-
rc_d.*sqrt(3)./4).*rc_d+3.*(pi./8.*rc_d.^2));
rc_v = 3.*(pi./4.*rc_d.^2).*(install_draft-bb_h); % For all three radial
columns
cc_v = pi./4.*cc_d.^2.*(install_draft-bb_h);
displaced_v = bb_v+rc_v+cc_v;

% RNA Mass Properties (t)

blade_m = (3.07.*rotor_d^1.83)./1e3;
hub_m = (0.23.*rotor_d^2.46)./1e3;
rotor_m = (5.*rotor_d^2.05)./1e3;
nacelle_m = (24.3.*rotor_d^1.88)./1e3;
rna_m = rotor_m+nacelle_m;

% Tower Properties

hub_h = 0.47.*rotor_d+31; % (m)
tower_m = 1263.*p_xy^2; % (t) Baseline tower mass is 1263t
tower_com = hub_h./(150./56.5); % (m) Same ratio as baseline

% Hull Mass Properties (t)

fixhull_m = p_xy^2.*6454; % Baseline fixed mass is 6454t
fixsys_m = rna_m+tower_m+fixhull_m;
waterballast_3m = ((ocean_rho.*(pi./4.*(3.*rc_d.^2+cc_d.^2)).*(install_draft-
bb_h)+(ocean_rho.*bb_v))-(fixsys_m.*1000))./1000; % for all three legs
%concreteballast_3m = p_xy^2.*2540; % Baseline concrete ballast
mass is 2540t, for all three columns
concreteballast_3m = fixhull_m*2540/6454;
hullsteel_m = p_xy^2.*3914; % Baseline steel mass is 3914t
totalhull_m = fixhull_m+waterballast_3m; % with ballast

% System Mass Properties (t)

totalsys_m = totalhull_m+rna_m+tower_m;

% Area Moment of Inertia of Water Plane Area (m^4)

waterplane_Iy =
(pi./4.*(cc_d./2).^4)+(pi./4.*(rc_d./2).^4+(pi./4.*rc_d.^2).*radial_spacing.^2
)+2.*(pi./4.*(rc_d./2).^4+(pi./4.*rc_d.^2).*(radial_spacing.*(sind(30))).^2);

% Center of Buoyancy (m)

cob = (((-install_draft+bb_h)./2.*(rc_v+cc_v))+((-
install_draft+bb_h./2).*bb_v))./(displaced_v);

```

```

% Thrust Force Scaling (N)

thrust_N = 84.*rotor_d^1.86;

% Moment of Inertia Calculations

column_h = (install_draft+freeboard);

steel_rho = 7850;      % (kg./m^3)
steel_t =
hullsteel_m.*1000./((3.*(rc_d.*pi.*column_h+pi./2.*rc_d.^2)+3.*(2.*bb_h.*bb_l+
2.*rc_d.*bb_l)+(cc_d.*pi.*column_h+pi./2.*cc_d.^2)).*steel_rho); % (m) Steel
thickness calculated by dividing hull steel mass by the product of steel
density and hull surface area

concrete_rho = 2400;   % (kg./m^3)
waterballast_hi = (waterballast_3m./3).*1000./(ocean_rho.*bb_l.*rc_d); %(m)
[m,n,o] = size(waterballast_hi);
waterballast_h=zeros(m,n,o);

for i=1:m
    for j = 1:n
        for k = 1:o
            if waterballast_hi(i,j,k) <= bb_h(i,j,k)
                waterballast_h(i,j,k) = waterballast_hi(i,j,k);
            else
                waterballast_h(i,j,k) = bb_h(i,j,k);
            end
        end
    end
end

waterballastrc_3m = zeros(m,n,o);

for i=1:m
    for j = 1:n
        for k = 1:o
            if waterballast_hi(i,j,k) <= bb_h(i,j,k)
                waterballastrc_3m(i,j,k) = 0;
            else
                waterballastrc_3m(i,j,k) = waterballast_3m(i,j,k)*1000-
3.*rc_d(i,j,k)*bb_l(i,j,k)*bb_h(i,j,k)*ocean_rho; %kg
            end
        end
    end
end

waterballastrc_h = waterballastrc_3m./3./(ocean_rho.*pi./4.*rc_d.^2);

concreteballast_h =
concreteballast_3m.*1000./3./(pi./4.*rc_d.^2.*concrete_rho); %(m)

bb_m = (2.*(rc_d.*bb_l)+2.*(rc_d.*bb_h)+2.*(bb_l.*bb_h)).*steel_t.*steel_rho ;
%(kg)
bb_xcg = radial_spacing./2;

```

```

bb_zcg = -install_draft+bb_h./2; % relative to z=0

cc_m =
((cc_d./2).^2.*pi.*2+(install_draft+freeboard).^2.*pi.*cc_d./2).*steel_t.*steel_rho ;
cc_xcg = 0 ;
cc_zcg = -install_draft+(install_draft+freeboard)./2;

rc_m =
((rc_d./2).^2.*pi.*2+(install_draft+freeboard).^2.*pi.*rc_d./2).*steel_t.*steel_rho ;
rc_xcg = radial_spacing;
rc_zcg = -install_draft+(install_draft+freeboard)./2;

waterballast_m = waterballast_3m./3.*1000;
waterballast_xcg = radial_spacing./2;
waterballast_zcg = -install_draft+waterballast_h./2;

waterballastrc_m = waterballastrc_3m./3;
waterballastrc_xcg = radial_spacing;
waterballastrc_zcg = -install_draft+concreteballast_h+waterballastrc_h./2;

concreteballast_m = concreteballast_3m./3.*1000;
concreteballast_xcg = radial_spacing;
concreteballast_zcg = -install_draft+concreteballast_h./2;

totalhull_com =
(3.*bb_m.*bb_zcg+cc_m.*cc_zcg+3.*rc_m.*rc_zcg+3.*waterballast_m.*waterballast_zcg+3.*waterballastrc_m.*waterballastrc_zcg+3.*concreteballast_m.*concreteballast_zcg)./(totalhull_m.*1000);

totalsys_com =
(rna_m.*hub_h+tower_m.*tower_com+totalhull_m.*totalhull_com)./totalsys_m;

towerinterface_m = 100000; %(kg)
towerinterface_zcg = freeboard;

tower_mkg = tower_m.*1000;
tower_zcg = tower_com;

nacelle_mkg = nacelle_m.*1000;
nacelle_zcg = hub_h;

rotor_mkg = rotor_m.*1000;
rotor_zcg = hub_h;

bb_zcgo = bb_zcg - totalsys_com;
cc_zcgo = cc_zcg - totalsys_com;
rc_zcgo = rc_zcg - totalsys_com;
waterballast_zcgo = waterballast_zcg - totalsys_com;
waterballastrc_zcgo = waterballastrc_zcg - totalsys_com;
concreteballast_zcgo = concreteballast_zcg - totalsys_com;
towerinterface_zcgo = towerinterface_zcg - totalsys_com;
tower_zcgo = tower_zcg - totalsys_com;
nacelle_zcgo = nacelle_zcg - totalsys_com;

```

```

rotor_zcgo = rotor_zcg - totalsys_com;

% Calculated Mass

fixhull_calc = (3*(bb_m+rc_m+concreteballast_m)+cc_m)/1000; %(t)
fixsys_mcalc = rna_m+tower_m+fixhull_calc; %(t)
waterballast_3mcalc =
((ocean_rho.*(pi./4.*(3.*rc_d.^2+cc_d.^2)).*(install_draft-
bb_h)+(ocean_rho.*bb_v))-(fixsys_mcalc.*1000))./1000; % (t) for all three legs
totalhull_mcalc = fixhull_calc+waterballast_3mcalc; % (t) with ballast

totalsys_mcalc = totalhull_mcalc+rna_m+tower_m; %(t)
%

cc_ICGy = cc_m./12.*(6.*(cc_d./2).^2+(install_draft+freeboard).^2);
rc_ICGy = rc_m./12.*(6.*(rc_d./2).^2+(install_draft+freeboard).^2);
waterballast_ICGy = 1./12.*waterballast_m.*(waterballast_h.^2+rc_d.^2);
waterballastrc_ICGy =
1./4.*waterballastrc_m.*(rc_d./2).^2+(1./12.*waterballastrc_m.*waterballastrc_
h.^2);
concreteballast_ICGy =
1./4.*concreteballast_m.*(rc_d./2).^2+(1./12.*concreteballast_m.*concreteballa
st_h.^2);

tower_ICGy = 1./12.*tower_mkg.*(6.*(tower_d/2).^2+(hub_h-freeboard).^2);
rotor_ICGy = 1./4.*rotor_mkg.*(rotor_d./2).^2;

cc_a = cc_m.*cc_xcg.^2;
rc_a = rc_m.*rc_xcg.^2;
waterballast_a = waterballast_m.*waterballast_xcg.^2;
waterballastrc_a = waterballastrc_m.*waterballastrc_xcg.^2;
concreteballast_a = concreteballast_m.*concreteballast_xcg.^2;

cc_b = cc_m.*cc_zcgo.^2;
rc_b = rc_m.*rc_zcgo.^2;
waterballast_b = waterballast_m.*waterballast_zcgo.^2;
waterballastrc_b = waterballastrc_m.*waterballastrc_zcgo.^2;
concreteballast_b = concreteballast_m.*concreteballast_zcgo.^2;
towerinterface_b = towerinterface_m.*towerinterface_zcgo.^2;
tower_b = tower_mkg.*tower_zcgo.^2;
nacelle_b = nacelle_mkg.*nacelle_zcgo.^2;
rotor_b = rotor_mkg.*rotor_zcgo.^2;

cc_Iy = cc_ICGy+cc_a+cc_b;
rc_Iy = rc_ICGy+rc_a+rc_b;
waterballast_Iy = waterballast_ICGy+waterballast_a+waterballast_b;
waterballastrc_Iy = waterballastrc_ICGy+waterballastrc_a+waterballastrc_b;
concreteballast_Iy = concreteballast_ICGy+concreteballast_a+concreteballast_b;
towerinterface_Iy = towerinterface_b;
tower_Iy = tower_ICGy+tower_b;
nacelle_Iy = nacelle_b;
rotor_Iy = rotor_ICGy+rotor_b;

bb_SA = 2.*bb_l.*bb_h+2.*bb_l.*rc_d+2.*bb_h.*rc_d;

```

```

ab_m = bb_l.*bb_h./bb_SA.*bb_m;
ac_m = bb_l.*rc_d./bb_SA.*bb_m;
bc_m = bb_h.*rc_d./bb_SA.*bb_m;

bb_ICGy =
2.*((1./12.*ab_m.*(bb_l.^2+bb_h.^2))+(1./12.*ac_m.*(bb_l.^2)+ac_m.*(bb_h./2).^
2)+(1./12.*bc_m.*(bb_h.^2)+bc_m.*(bb_l./2).^2));
bb_a = bb_m.*bb_xcg.^2;
bb_b = bb_m.*bb_zcgo.^2;

bb_Iy = bb_ICGy+bb_a+bb_b;

totalsys_Iy =
1.5.*(rc_Iy+waterballast_Iy+waterballastrc_Iy+concreteballast_Iy+bb_Iy)+cc_Iy+
towerinterface_Iy+tower_Iy+nacelle_Iy+rotor_Iy;

% Added Mass

addedmass_c = 1.36+(((rc_d./bb_l)-2)./(1-2)).*(1.51-1.36);

bb_ampl = addedmass_c.*pi.*(rc_d./2).^2.*ocean_rho;
cc_ampl = ocean_rho.*pi./4.*cc_d.^2;
rc_ampl = ocean_rho.*pi./4.*rc_d.^2;

bb_am = bb_ampl.*radial_spacing;
cc_am = cc_ampl.*install_draft;
rc_am = rc_ampl.*install_draft;

bb_amxCG = radial_spacing./2;
rc_amxCG = radial_spacing;

bb_amzCG = -install_draft+bb_h./2;
cc_amzCG = -install_draft./2;
rc_amzCG = -install_draft./2;

bb_amzCGo = bb_amzCG - totalsys_com;
cc_amzCGo = cc_amzCG - totalsys_com;
rc_amzCGo = rc_amzCG - totalsys_com;

bb_amICGy = 1./12.*bb_am.*(bb_h.^2+bb_l.^2);
cc_amICGy = 1./4.*cc_am.*(cc_d./2).^2+1./12.*cc_am.*install_draft.^2;
rc_amICGy = 1./4.*rc_am.*(rc_d./2).^2+1./12.*rc_am.*install_draft.^2;

bb_ama = bb_am.*bb_amxCG.^2;
rc_ama = rc_am.*rc_amxCG.^2;

bb_amb = bb_am.*bb_amzCGo.^2;
cc_amb = cc_am.*cc_amzCGo.^2;
rc_amb = rc_am.*rc_amzCGo.^2;

bb_amIy = bb_amICGy+bb_ama+bb_amb;
cc_amIy = cc_amICGy+cc_amb;
rc_amIy = rc_amICGy+rc_ama+rc_amb;

```



```

totalam_Iy = 1.5.*bb_amIy; %for small angles, the columns only move up and
down so no contribution to heave

% Results

pitch_stiffness = ocean_rho.*g.*waterplane_Iy+ocean_rho.*g.*displaced_v.*cob-
totalsys_m.*1000.*g.*totalsys_com;

pitch_deflection_rad = (thrust_N).*(hub_h-fairlead)./pitch_stiffness;

pitch_deflection_deg = pitch_deflection_rad.*360./(2.*pi);

pitch_natural_f = sqrt(pitch_stiffness./(totalsys_Iy+totalam_Iy))./(2.*pi);

pitch_period = 1./pitch_natural_f;

heave_natural_f =
sqrt(ocean_rho.*g.*waterplane_a./(3.*bb_am+totalsys_m.*1000))./(2.*pi);

heave_period = 1./heave_natural_f;

towout_m = fixsys_m;

towout_draft_i = (towout_m.*1000./ocean_rho-
bb_v)./(pi./4.*(3.*rc_d.^2+cc_d))+bb_h;
towout_draft = zeros(m,n,o);

for i=1:m
    for j = 1:n
        for k = 1:o
            if towout_draft_i(i,j,k) > bb_h(i,j,k)
                towout_draft(i,j,k) = towout_draft_i(i,j,k);
            else
                towout_draft(i,j,k) =
(towout_m*1000/ocean_rho)/(sqrt(3)/4*rc_d(i,j,k)^2+3*(radial_spacing(i,j,k)-
rc_d(i,j,k)*sqrt(3)/4)*rc_d(i,j,k)+3*(pi/8*rc_d(i,j,k)^2));
            end
        end
    end
end

max_width = 2.*(radial_spacing+rc_d./2).*sind(60);

%% Minimum Mass Search

minmass = 10000000;

for i=1:m
    for j = 1:n
        for k = 1:o

            if totalsys_m(i,j,k) < minmass && pitch_deflection_deg(i,j,k) < 7
&& pitch_period(i,j,k) > 25 && heave_period(i,j,k) > 18 && max_width(i,j,k) <
100 && towout_draft(i,j,k) < 10

```

```

        minmass = totalsys_m(i,j,k);
        U = i;
        V = j;
        W = k;

        else minmass = minmass;
        end

    end
end
end

%% Record Data in Table

sz = [1 10];
varTypes =
["double","double","double","double","double","double","double","double","double","double"];
varNames = ["Turbine Size","Minimum Mass","Radial Column Diameter", "Radial Spacing", "Bottom Beam Height", "Pitch Deflection", "Pitch Period", "Heave Period", "Maximum Floater Width", "Towout Draft"];
tblstudy = table('Size',sz,'VariableTypes',varTypes,'VariableNames',varNames);

tblstudy(q,:) = {power_MW, minmass, rc_d(U,V,W), radial_spacing(U,V,W),
bb_h(U,V,W), pitch_deflection_deg(U,V,W), pitch_period(U,V,W),
heave_period(U,V,W), max_width(U,V,W), towout_draft(U,V,W)};

```

## AUTHOR'S BIOGRAPHY

Samuel W. Davis was born in Bar Harbor, Maine on April 8, 2001. He moved to Belfast, Maine at the age of five and grew up there, graduating from Belfast Area High School in 2019 as valedictorian. Moving on to the University of Maine in Orono, Sam is majoring in Mechanical Engineering. In the summer of 2021, he began working at UMaine's Advanced Structures and Composites Center (ASCC) for the Offshore Wind Team, where he was first introduced to the field of research. For his Senior Capstone project, his team has designed and is in the process of constructing a small wind turbine.

Upon graduation, Sam will begin working on his master's degree in mechanical engineering at UMaine with Dr. Amrit Verma. The master's research will involve the installation and marine operations related to state-of-the-art floating offshore wind turbines designed by the ASCC.